INSTITUTE FOR OIL SANDS INNOVATION AT THE UNIVERSITY OF ALBERTA
Breakthrough Energy Research | Advanced Environmental Technologies

Imperial ALBERTA INNOVATES FACULTY OF ENGINEERING

IOSI PROJECT FINAL REPORT

Project Number	IOSI 2016-06
Project Title	Non-thermal plasma assisted catalytic bitumen partial upgrading under methane environment
Project Budget and Tenure	$240,000 October 1, 2017 ~ March 31, 2020
Principal Investigators	Dr. Hua Song, University of Calgary, sonh@ucalgary.ca
HQP	Dr. Aiguo Wang, Postdoctoral Fellowship Dr. Jonathan Harrhy, Postdoctoral Fellowship Shijun Meng, Ph.D. Candidate
Industrial Stewards	Sepideh Mortazavi Manesh, Imperial Oil Murray Gray, Alberta Innovates
Report Prepared by	Dr. Hua Song
Date	July 20, 2020

DISCLAIMERS

EXECUTIVE SUMMARY

Hydrocracking is conventionally employed as the process to upgrade bitumen for reduced viscosity and density as well as other property enhancements. Such process is costly and energy inefficient due to the involvements of expensive hydrogen and severe reaction conditions. Compared to hydrotreating, plasma assisted methane treating is more environmentally friendly and economically profitable. This research aims to develop a cost-effective partial upgrading technology. This research explored the possibility to apply a technology based on the directly catalytic incorporation of natural gas into bitumen at mild condition under the facilitation of in situ generated non-thermal plasma. However, upgrading of heavy oil model compound with ring structure shows unpromising outcome. The results indicate the aromatics is difficult to activate by plasma, while the ring of aromatics is hard to open.

In the meanwhile, the reactions with dodecane and decene imply that cracking, C-C coupling, and hydrogenation are the dominant reactions. These observations suggest this technology is very effective for gas phase reaction, carbon chain extension, and olefin reduction, which inspire us to apply NTP technology on light hydrocarbon utilization. Therefore, except bitumen related study, more research effort has been focused on the gas phase reaction, such as the conversion of light hydrocarbons (biogas, natural gas, LPG) to valuable liquid chemicals. Biogas can be converted to more valuable liquid chemicals such as formaldehyde, methanol, ethanol, and acetone rather than syngas; light hydrocarbons such as natural gas and LPG can be transformed to C_6-C_9 branched-chain alkanes at low temperature and atmospheric pressure.

These findings provide an environmentally superior option to meet rapidly growing energy demands. From the viewpoint of engineering practice, one pot process developed in this project has the potential to make the utilization of natural gas more economically profitable. Moreover, the achievement made from this project will further ascertain the leading position of Canada in the world's energy market through more efficient and cleaner utilization of light hydrocarbon which are abundant natural resources in Canada.

TABLE OF CONTENTS

LIST OF FIGURES

LIST OF TABLES

1 INTRODUCTION

Hydrocracking is conventionally employed as the process to upgrade bitumen for reducing its viscosity and density, increasing its H/C ratio, and removing associated impurities. Such process is costly and energy inefficient due to the involvements of expensive hydrogen generated from a separate unit through natural gas steam reforming and high operation pressure.

This research aims to develop a cost-effective partial upgrading technology to increase the mobility of the bitumen extracted from surface minable oil sands. Reducing the viscosity will satisfy the pipeline transportation specification while enhancing the quality of the upgraded oil beneficial for its further refining at the other end of the pipeline. This will be done using a technology based on the directly catalytic incorporation of natural gas into bitumen at mild temperature and atmospheric pressure under the facilitation of in situ generated plasma in a nonthermal way. The in situ activated and ionized methane then interacts with the broken molecular pieces formed from bitumen thermal cracking with the assistance of high voltage electric field, leading to the production of the partially upgraded oil with enhanced oil yield and quality for pipeline transportation under the facilitation of co-existing catalyst.

Compared to hydrotreating, plasma assisted methane treating is more environmentally friendly and economically profitable. Moreover, the achievement made from this project will further ascertain the leading position of Canada in the world's energy market through more efficient and cleaner utilization of heavy crude oil and natural gas which are abundant natural resources in Canada.

Research objectives include:

- Determine the optimal reactor configuration for non-thermal plasma (NTP) generation at lab scale.
- Identify the effect of NTP addition on bitumen partial upgrading and determine the optimized plasma generation conditions and reaction conditions.
- Deliver at least one catalyst formulation which can effectively catalyze bitumen partial upgrading using methane to produce pipeline quality crude oil under the facilitation of the non-thermal plasma.
- Identify the effect of NTP addition on the catalytic liquefaction of other hydrocarbon resources (e.g. natural gas, LPG, biogas).
- Gain a better understanding of the non-thermal assisted plasma-catalytic reaction mechanism beneficial for kinetic model development.
- Determine the economic feasibility of this novel non-thermal plasma methane assisted catalytic bitumen partial upgrading technique at commercial scale using process simulation.

To reach the mentioned objectives, the performed studies and major results are summarized as follows:

- Catalytic assisted Direct Barrier Discharge (DBD) reactor has been developed and tested for both gas and gas-liquid reactions. Optimal conditions for safe plasma generation has been established.

- Upgrading of 1-methylnaphthalene chosen as a heavy oil model compound study for liquid substrate testing shows unpromising performance, and the data indicates very little synergy between the catalytic and plasma reactions because the liquid substrate is hardly activated by plasma.
- More investigations on the plasma reactions of other heavy oil model compounds, cyclohexane, toluene, dodecane and decene, at gas phase are carried out. The results of the conversion of cyclohexane and toluene suggest that the ring is hard to open, and ring alkylation is the major reaction under the plasma conditions. The reactions with dodecane and decene imply that cracking, C-C coupling, and hydrogenation are the dominant reactions. These observations suggest this technology is very effective for gas phase reaction, carbon chain extension, and olefin reduction.
- Catalytic dry reforming of methane has been thoroughly investigated as a model reaction for initial investigations, including analytical methods for thorough analysis of gas, liquid and coke products investigated to obtain a closed carbon balance, numerous catalysts designed and investigated to increase conversion of CH_4 and CO_2, increase selectivity towards liquid products (rather than syngas) and minimize coke deposition.
- The investigations of simulated natural gas and liquified petroleum gas show that C_1-C_4 light hydrocarbons are effectively converted into C_6-C_9 branched-paraffins with high yield and low coke formation. The statistically significant synergetic interactions between the catalyst and plasma are observed during the conversion of light hydrocarbons into liquid chemicals.
- One unique photocatalyst Ti-Ga/UZSM5 is developed. This catalyst could utilize the UV/Visible light generated from plasma, thus significantly increase the conversion, improve the liquid yield, and control the coke formation.
- These results were published on Energy Conversion and Management, The Journal of Physical and Chemistry Letters, and Chemical Communications.

Two postdoctoral scholars specialized in oil upgrading and heterogeneous catalysis along with a doctoral student were engaged in this project full time. They were trained to become not only a quick learner for new area in this project, but also independent researchers with critical thinking ability. All these researchers were given many opportunities to develop their experimental, technical communication and academic writing skills.

2 BACKGROUND

There are an estimated 174 billion barrels of natural bitumen reserves in Canada. In 2016, bitumen production from the oil sands was ~2.5 million barrels per day (bpd). The Canada's National Energy Board has projected that bitumen production will jump to 4.3 million bpd by 2040. The extracted bitumen from oil sands has an average density of 1.0077 g/cm^3, API gravity of 8.9, and a dynamic viscosity of 2×10^5-2×10^6 cP at atmospheric conditions[1]. Such bitumen is highly viscous and must be diluted to meet pipeline specifications for transport to refineries in the United States. Pipeline transport requires a fluid density of < 0.940 g/cm^3 and dynamic viscosity of < 330 cP (at 7.5-17 ℃)[1, 2]. As such, the goal of this project is to develop a process that can reduce the viscosity and increase the API of bitumen to meet pipeline specifications in a more economical way.

Traditionally hydroconversion processes can be used to decrease the viscosity of oil, improve the API gravity, and reduce the S content of the oil. Using hydrogen in bitumen upgrading is well known and can enhance the properties of the oil, but the costs of hydroconversion are relatively high due to the consumption of high pressure H_2 (>8 MPa) [3]. An alternative approach to obtain the benefits of hydrogen addition is to add a cheap and abundant H-donor to the bitumen, such as methane. The goal of the current project is to develop a partial upgrading technology to increase the mobility of the extracted bitumen by reduction of the viscosity. This will be done using a technology based on the non-thermal plasma assisted catalytic incorporation of natural gas (i.e. methanoconversion) into cracked bitumen at mild temperature and 1 atm compared to hydroconversion (i.e. 400 ℃ and 16 MPa H_2) as natural gas prices are far more economically advantageous compared to H_2.

The use of methane to upgrade crude oil is not a novel idea. However, based on a thorough literature search the work surrounding this area is limited and dominated by one research group headed by Cesar Ovalles. As shown by their work [4-6], the conversion and viscosity reduction of extra-heavy crude oil over typical dispersed Fe and Mo catalysts in a methane atmosphere is poor. Consequently, this may be the reason why limited development or progress has been made in this area in recent years. Subsequently, there is a need for further research in this area for better methane activation to achieve more efficient methanotreating.

Compared to hydrogen, methane has much more stable molecular structure (tetrahedron), resulting in its inert chemical and physical properties. Therefore, the developed catalyst should activate the methane first to make it as active as hydrogen for participating into the cracked bitumen upgrading process. The methane activation is triggered by the first C-H bond cleavage in its tetrahedral structure. Such bond breakage requires activation energy as high as 104 kcal/mol. However, once the first C-H bond is broken, the formed methyl radical is very active, and the remaining C-H bonds cleavage will happen automatically in a chain reaction if there is no termination group to end it. The desired catalyst should be able to effectively lower down the energy barrier allowing the methane activation happening at less severe reaction conditions.

Traditional thermo-catalytic methods employ both oxidative [7, 8] and non-oxidative [9, 10] conditions to yield olefins and aromatics whereas partial oxidation of methane with carbon dioxide forms valuable syngas.[11, 12] Firstly, the methane activation has been extensively studied under oxidative environment, which is thermodynamically favored, through so-called oxidative coupling of methane (OCM) reaction to produce ethylene, a very important petrochemical feedstock, since 1980s. Although hundreds of catalysts which have been comprehensively reviewed [13-16] have been tested since then, their poor C_2 product yields (<25%) limit the further commercial

considerations of such process. Under such circumstance, rather than keeping trying to optimize catalyst formulation for slightly enhanced performance which might be internally limited by the reaction thermodynamics as hinted by the empirical rule of 100 [17], many researchers have dedicated themselves to the field of methane activation under nonoxidative condition over the past more than thirty years and many catalyst systems have been reported [18-24], among which zeolite supported molybdenum catalyst demonstrates the most promising activity toward methane conversion to higher hydrocarbons [25]. Even though, less than 10% methane conversion is observed when the temperature is higher than 700 ℃ with major products in aromatics. Obviously, this category of catalysts cannot meet the requirements raised from the methanotreating process either.

We need to thank the promising work pioneered by Choudhary, et al. [26] and evidenced by a series of following publications [27-29] which indicates that methane conversion will be significantly improved in the presence of higher hydrocarbon reactants, particularly unsaturated hydrocarbons at much lower temperature region (400 ~ 600 ℃) and atmospheric pressure and which sets the partial ground for this proposed technology. Based on these observations, the co-existing heavy oil which is primarily composed of higher hydrocarbons including paraffins, aromatics, and naphthenes [30] should help the activation of methane and its following conversion after its initial crack down to smaller molecules containing shorter carbon chain aided by the co-existing cracking catalyst. The activated methane molecule will form CH_x and H_{4-x} species. Hydrogen species will then be used for cracking down the aromatic ring and attached long side carbon chain and following saturation through hydrogenation and hydrogenolysis reactions while removing sulfur, nitrogen, and metal out from the crude oil under the facilitation of the developed catalyst. At the same time, the cracked heavy oil molecules should be able to react with the produced CH_x moiety to form more synthetic crude oil. Therefore, theoretically speaking, the synergetic effect between heavy oil and methane during methanotreating process should take place when suitable catalyst system is charged, which has been experimentally evidenced by the previous studies performed in our research group related to heavy oil upgrading supported by the last Imperial Oil and CRD joint funding [31-34], light olefin upgrading [35-38], and biomass upgrading [39-42] as highlighted in the "Contributions" section of the Form 100. Moreover, the methane engagement into the upgrading reaction and incorporation into the formed products has also been successfully witnessed. However, the measured methane conversion still remains lower than 10% even under the best scenario.

Many attempts are made to activate methane in a non-traditional way. Non-thermal plasma (NTP) is an exciting and emerging technology within light hydrocarbon utilization towards value-added chemicals, which allows thermodynamically unfavorable chemical reactions to readily proceed at relatively low temperature in a non-equilibrium approach.

Versatile discharge techniques such as corona discharge, spark discharge, microwave discharge, gliding arc discharge, and dielectric barrier discharge (DBD) have been developed for generating different methane plasma sources with their own characteristics of electron energy and degree of thermal activation, leading to different product distribution [43]. For example, the main product of a methane DBD is typically ethane, with a non negligible amount of propane and butane. However, in the case of a spark discharge, acetylene selectivity is significantly increased. The formed non-thermal methane plasma (also called non-equilibrium plasma) is characterized by the presence of electrons that have much higher energy than the other surrounding particles, as a result of which there is a huge temperature difference between these electrons and background gas. The temperature of the electrons can be as high as 10^5 K while the reactive gas still

maintains at the reaction temperature [43-45]. These generated highly energetic electrons make collisions with the surrounding methane gas molecules and then produces CH_x and H species as well as corresponding ion species (e.g. CH_x^+) which are active for bitumen upgrading.

In addition to the innumerous catalytic methane activation attempts, plasma assisted methane activation has also been extensively studied by many researchers over the past more than 30 years upon applying high temperature (>2,300 K) [46] in a thermal way or high voltage electric field (e.g., 10-20 kV) [44] in a non-thermal approach to generate plasma state methane composed of positive, negative ions, electrons, and neutral species [46] which are chemically active for its following conversion to form versatile valuable products such as high purity hydrogen, carbon with nanostructure, synthesis gas, and higher hydrocarbons. Compared to thermal one, non-thermal plasma assisted methane activation is more energy efficient and more applicable for bitumen upgrading because the reaction temperature can be maintained at relatively low level to effectively prevent overcracking.

The aforementioned catalyst assisted synergetic effect on methane activation can be further enhanced when an external electric field at high voltage is applied in a non-thermal way. The resulting formed plasma state methane is much more chemically active and can readily participate in the catalytic bitumen partial upgrading for producing pipeline transportable crude oil. Such so-called hybrid catalytic-plasma strategy for methane activation and conversion has been repeatedly reported by many researchers in the literature for the formations of hydrogen, higher hydrocarbons, synthesis gas, and clean gas from after-treatment of exhaust gas.

For example, according to the report from Heintze et al. [47], methane conversion was significantly increased from 7% to 25% at 300 °C during its partial oxidation when plasma power was applied to the Ni/Al_2O_3 catalyst bed in a DBD mode. A similar promotion effect is also witnessed by Liu et al. where an increase of methane conversion from 4.3% to 27.4% was noticed after $Sr-La_2O_3/La(OH)_3$ catalyst was introduced into a corona discharge environment for higher hydrocarbon production [48]. Moreover, for methane reforming reaction, the synergistic factor, defined as the ratio of the performance achieved with plasma catalysis to the summation of the performance obtained with plasma-alone and catalysis-alone, can be as high as 2.4 [49]. Therefore, the synergism is highly expected to be observed during our proposed upgrading reaction, which originates from the interactions between plasma and catalysis.

There are also a few papers dedicated to the study of non-thermal assisted heavy oil upgrading at elevated temperature under atmospheric pressure gas flow [50-52]. It is observed that the gas reactivity can be promoted by exciting to its plasma state, which can in turn accelerate heavy oil conversion to gas and light oil products through intimate gas/liquid interaction. However, the inherent poor product selectivity under plasma conditions limits the wide implementation of this technique. Therefore, there is an intrinsic need for the combination of catalyst and non-thermal plasma operation for enhancing heavy oil upgrading performance under methane environment in order to meet the pipeline transportation specifications with maximized liquid yield.

Kong, et al. patented a non-thermal plasma system with optional catalyst loading and UV lighting accessories and corresponding method for natural gas and heavy hydrocarbon co-conversion [53], which disseminates a similar concept as what has been disclosed in the proposed research. Nevertheless, the plasma-catalytic effect and methane participation are not demonstrated at all from the reported experimental results, since the data collected from the control runs are not provided where no plasma power is applied with and without catalyst addition under N_2 or CH_4 environment. Moreover, the reported conventional hydrotreating

catalyst in this patent might not have any effect on methane activation. It is even more frustrating that there are no following publications from the organization reporting the experimental details and continuous study on this topic.

Application of an electric field generates highly energetic electrons with a typical electron temperature of 1-10 eV, such species may transform inert molecules into excited states through ionization, vibrational and rotational excitation and radical formation,[54] thus initiating various chemical reactions at far lower temperatures (e.g. room temperature) compared with thermal catalysis owing to high thermodynamic barrier. Therefore, NTP technology can be applied to other reactions. For example, dry reforming of CH_4 (DRM) with CO_2 to syngas [55-59] ($CH_4+CO_2 \rightarrow 2CO+H_2$, ΔH_{298K}=247 kJ/mol).

The synergistic effect between NTP and the catalyst was also observed in DRM with CO_2 into syngas at room temperature. [58, 60-63] The selectivity of C_2-C_4 hydrocarbons from methane conversion increases when using the catalyst in the plasma reaction.[64] The same positive effect on the formation of liquid chemicals is reported in one-step reforming of CO_2 and CH_4.[65] Catalyst development for the hybrid plasma-catalytic system has focused primarily on γ-Al_2O_3 supported Ni,[65-71] Cu,[65, 72] Ag,[64] Pd [73, 74], Pt [65], and Rh [75], with few studies on zeolite catalyst [55, 76-78].

Biogas is a promising renewable energy source, which primarily consists of methane (55-65%) and carbon dioxide (35-45%) [79] produced from the anaerobic digestion of biomass, landfill, and wastewater treatment. Extensive investigations on the conversion of biogas with NTP are mostly concentrated on producing syngas or higher hydrocarbons (C_2-C_4) [55, 58, 66, 70, 80], while very little effort is devoted to the formation of liquid products.[65] Another critical issue for a plasma-catalytic reaction is the formation of carbonaceous species, which are both a waste of raw materials and poisonous to the catalyst. Carbonaceous species is largely overlooked within plasma-assisted catalytic DRM reported in the literature and predominantly estimated to be higher than 10%. [65, 66] Actually, the coke yield is more severe. Importantly, the nature of carbonaceous species has a significant effect upon the plasma itself, with more stable carbon species (oxidized at T>650K) destabilizing the plasma resulting in arcing and poorer methane conversion.[81] On this note, we herein employ NTP to simultaneously converted biogas to liquid chemicals with controlled carbon deposition at low temperature and atmospheric pressure.

Light hydrocarbons, including natural gas and liquefied petroleum gas (LPG), are abundant, cheap and underutilized. Natural gas is mainly used for residential heating, cooking, and electricity generation. LPG is manufactured in the process of petroleum (crude oil) refining or extracted from petroleum or natural gas stream as they emerge from the ground, which generally consists of hydrocarbons with three and/or four carbon atoms. LPG is commercially used as a fuel in heating appliances and cooking equipment. The high-octane rating and less CO_2 emission enable LPG to be widely employed as a vehicle fuel, thus lowering dependence on petroleum based liquid fuels and reducing the environmental concerns. [82] Besides, LPG with high-grade purity is increasingly utilized as an aerosol propellant or a refrigerant [83], serving as a functional replacement for chlorofluorocarbon or hydrofluorocarbon refrigerant in an effort to reduce ozone depletion.

Extensive thermo-catalytic approaches are developed to convert natural gas to syngas [11], higher hydrocarbons [84], oxygenate chemicals [85], and aromatics [10] in an oxidative or non-oxidative way. In addition to convert LPG to light olefins (C_2H_4, C_3H_6) [86] and single-walled carbon nanotubes, [87] some attempts focus on steam reforming of LPG to produce hydrogen for fuel cells. [88] More

effort is devoted to the direct transformation of LPG to aromatics to increase its value. [89-91] Aromatics, particularly, BTX (benzene, toluene, xylene), are more valuable and can be used as the raw material in the petrochemical industry or blended with gasoline to enhance the octane number. [92] Unfortunately, light alkanes are chemically inert, which makes these transformations thermodynamically unfavourable at low temperatures. Conventional thermo-catalytic approaches to achieve these reactions require high reaction temperatures (> 673 K), which inevitably give less desired products with severe coke formation. [93]

Another direction being taken to break the high thermodynamic barrier for methane activation is photocatalysis, which employs photoenergy to promote reactions at low temperatures. Such low temperature could minimize the energy consumption and reduce the side reactions such as coke formation.[94] Photo-oxidative dehydrogenation of methane under simulated sunlight irradiation could generate C_2 hydrocarbons, and a selectivity of 89.47% for ethane can be obtained. [95] Upon photoirradiation with UV/vis, methane can undergo dehydrogenative coupling reaction to form ethane and hydrogen, [96, 97] and the selectivity of ethane and hydrogen products could be up to 99%. [97] It is also reported that methane can be photo-chemically converted to methanol and hydrogen in the presence of H_2O or CO_2 under the facilitation of UV-visible light. [98, 99] Despite the relatively high selectivity of products can be achieved under mild conditions, most of the reported photocatalytic conversions give a low product yield and a low energy efficiency.[94, 95]. Ultraviolet radiation can be self-generated by non-thermal dielectric barrier discharge plasma [100, 101] which drives us to integrate plasma activation and photocatalysis for light hydrocarbon conversion.

In summary, Alberta is rich in crude oil and ranked the third-largest crude oil reserve in the world. However, 99% of the reserved oil resource is heavy crude oil which needs to be significantly upgraded before customer use. With plasma activation, ionized methane will be effectively produced and then incorporated into bitumen upgrading process. Compared to hydrotreating, plasma assisted methane treating is more environmentally friendly and economically profitable. Because of the limited related research, the goa of this research is to identify the effect of NTP addition on bitumen partial upgrading under methane environment.

Canada is also abundant in natural gas reserves and is the third largest natural gas producer and exporter in the world. Increasing worldwide energy demand has sparked research interests towards the direct transformation of light hydrocarbons into valuable liquid fuels or chemicals.

It is reported that NTP technology could effectively activate light hydrocarbons for syngas or H_2 production. Another objective of this study is to achieve plasma assisted one-step catalytic liquefaction of light hydrocarbon.

In the meanwhile, a better understanding of the plasma-catalytic upgrading reaction and catalyst deactivation mechanism is very crucial to rationally design catalyst structure for achieving enhanced performance. Therefore, more thorough and in-depth investigation on this topic should be conducted to identify the role played by plasma and catalyst individually and how they jointly contribute to the bitumen partial upgrading under methane environment. More importantly, whether and how methane gets involved into the upgrading reaction need to be carefully examined.

3 EXPERIMENTAL

3.1 Non-thermal Plasma Reactor Configuration

Reactions were carried out in a coaxial dielectric barrier discharge (DBD) reactor at room temperature and atmospheric pressure (**Figure 1**). The DBD reactor consisted of a quartz tube and two coaxial electrodes. The inner high-voltage electrode was a stainless-steel rod with an outer diameter (o.d.) of 14.3 mm and installed along the axis of the quartz tube (25.4 mm o.d.×20.3 mm i.d.). The outer electrode is a copper coil (3.175 mm o.d.) wrapped on the external quartz tube served as the dielectric material. This configuration gives the discharge length of 80 mm with a discharge gap of 3 mm. The high voltage is applied to the inner electrode whereas the outer electrode is grounded. The pelleted catalyst is packed into the discharge area.

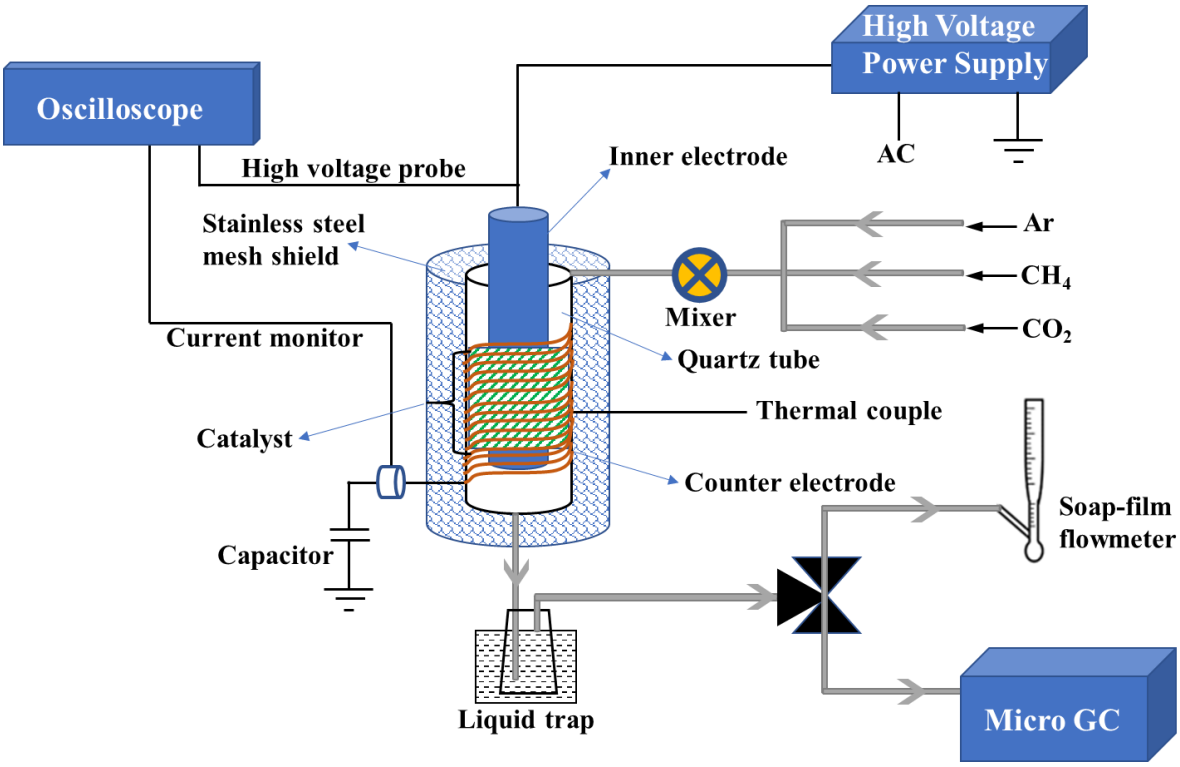

Figure 1. Schematic diagram of experimental setup

Depending on the position of catalyst, such interactions can be classified into two different categories (i.e., single-stage and two stage). The plasma-catalyst interactions become rather complicated once the catalyst is present within plasma zone. Such single-stage plasma catalysis could lead to three general technical advantages: (1) The charged catalyst enhances the energy efficiency of plasma chemistry due to its electric conductive feature, thus leading to the creations of more energized active species participating in the upgrading reaction. (2) The implementation of high voltage electric field increases the internal energy of reactants, the active metal dispersion on the catalyst support, and work function of the engaged catalyst, thus benefiting the improvement of catalytic reaction rate. (3) The metal dispersion enhancement could effectively suppress the coke formation and therefore alleviates the catalyst deactivation, thus extending catalyst durability [49].

The plasma discharge is generated using AC high-voltage generator (HVP, G2000). The voltage and current measurements are monitored with a two-channel digital oscilloscope (Tektronix, TBS2072) with 70 MHz bandwidth, 1 GS/s sample rate and 20 M record length. The oscilloscope equipped with an AC current probe (P6021A, Tektronix) with a bandwidth of 120 Hz to 60 MHz and a HV voltage probe (P6015A, Tektronix) with 75 MHz bandwidth and 40 kV maximum peak-to-peak voltage. All the experiments were conducted at ca. 9.25 kV peak to peak at load with a constant frequency of 17 kHz at room temperature.

To measure the reaction temperature, a thermocouple was put between quartz tube and outer electrode. The reaction temperature was around 100 ℃. The reaction temperature was also measured by an infrared thermal camera (FLIR ONE Pro), as shown in **Figure 2**. The camera was placed at 10 cm beneath the reactor to measure the temperature distribution of DBD reactor. The temperature was monitored after 40 min of reaction before the plasma is switched off. The average temperature of the entire reactor is 61.5 ℃, while the highest temperature is 96.9 ℃ on the inner electrode. These results indicate that the reaction is occurring at a relatively low temperature (< 100 ℃) during the whole reaction.

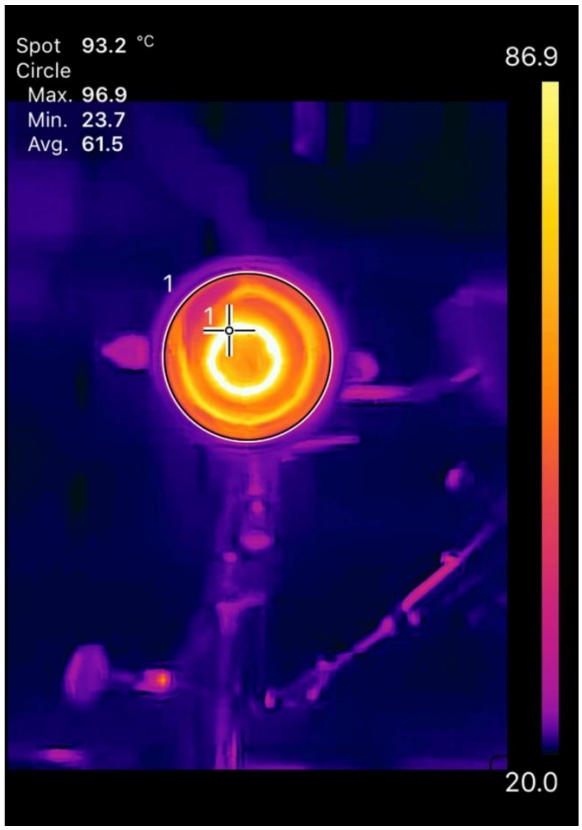

Figure 2. The measurement of reactor temperature by infrared camera after reaction

3.2 Catalyst Synthesis

According to the relevant literature and PI's previous research experiences on catalytic carbon source upgrading under methane environment [31-42], supported catalyst will be employed for this study, which is very different from the organometallic catalysts used in previous studies [5, 6]. Compared to its counterpart, the supported catalyst will make itself much easier to be recovered

from upgraded oil after reaction. Zeolite type support such as ZSM-5, zeolite A, zeolite Y, and zeolite beta with various Si:Al ratios and proper surface modification of phosphorus, alkali or alkali earth, and rare earth metals or Metal-Organic Frameworks (MOFs) type support such as MIL-140A, UiO-66, and MIL-53(Al) after the aforementioned surface modification will provide moderate acidity to catalytically crack down the introduced heavy oil while effectively preventing excessive cracking and coke formation. Mo, Ga, Zn, Ag, In, Pd, Ir, Pt, or their combinations will provide a good starting point as the active metal loaded on the aforementioned support for methane activation under the facilitation of co-added Sn, W, Fe, Co, or Ni as promoter. These active metals and/or promoters can be introduced into the framework of the selected support for effectively preventing its agglomeration, thus benefiting its better dispersion during the upgrading reaction for achieving better catalytic performance.

The commercial ammonium ZSM5 zeolite (CBV 8014) and HY zeolite (CBV 780) with Si/Al = 80 were purchased from Zeolyst. Ammonium ZSM5 was calcined at 600 ºC for 5 h in air to attain CZSM5(HZSM5) power.

UZSM5 zeolite support was prepared by hydrothermal synthesis. $Al(NO_3)_3 \cdot 9H_2O$ (98%, Alfa Aesar) was added to Tetrapropylammonium hydroxide (TPAOH, 1.0 M, Sigma Aldrich) stirred at room temperature (RT) until a clear solution was obtained. Tetraethyl orthosilicate (TEOS, Merck KGaA) was then added dropwise to the above solution. Amounts were calculated to obtain a molar ratio of Al_2O_3: $80SiO_2$: 21TPAOH: $943H_2O$ in the solution. The solution kept stirring at RT for 1h until the gel was obtained. The resulting supersaturated gel was transferred in an autoclave and held at 170 °C for 3 days. After cooling down to RT, the solid was recovered by centrifuge, dried at 90 °C for 12 h, ramped at 5 °C/min to 300 °C for 1 hour, then calcined in air at 600 ºC for 3h. The resultant powder was labeled as UZSM5. UZSM5 pellets and Pt/UZSM5 were prepared as described above.

γ-Al_2O_3 (Alfa Aesar, 200 $m^2 \cdot g^{-1}$) and SiO_2 (Alfa Aesar, 160 $m^2 \cdot g^{-1}$) catalyst supports were crushed into powder and screened with 100 mesh. The powder support (HZSM-5, UZSM-5, γ-Al_2O_3, SiO_2) was then mixed with LUDOX AM-30 colloidal silica, citric acid solution and methylcellulose with a mass ratio of 60powder catalyst: 4citric acid: $8H_2O$: 4methylcellulose: 45AM-30 colloidal silica. Then, the mixture was extruded into pellet. The extruded catalyst was calcined at 600 ºC for 5 h in air. The resulting sample was manually cut into pellets with a diameter of 2 mm and 5-10 mm in length.

Various metal species (Ag, Ga, Pt, Pd, Re, and Ir) were introduced on CZSM5 or UZSM5 via wet impregnation (WI). The precursors were $AgNO_3$ (99.0+%, Sigma-Aldrich), $Ga(NO_3)_3 \cdot xH_2O$ (99.9%, Sigma-Aldrich), $Pt(NH_3)_4(NO_3)_2$ (⩾50.0% Pt basis, Sigma-Aldrich), $Pd(NO_3)_2 \cdot 2H_2O$ (~40% Pd basis, Sigma-Aldrich), $ReCl_3$ (Sigma-Aldrich), $IrCl_3$ (⩾62% Ir, Alfa Aesar). WI was made by initially dissolving the corresponding amount (1wt.%) of precursor in 60.0 g deionized water, then 8.0 g pelleted CZSM5 was dispersed in the precursor solution and kept rotating (100 rpm) for 2 hours at 60 ºC on rotary evaporator. After that, water was completely evaporated at 60ºC. The wet catalyst was dried in the oven at 110 ºC overnight, followed by calcination at 550ºC with a heating rate of 5 °C/min and a holding time of 3 h in ambient air. The resulting catalysts were then stored properly for later use.

3.3 Characterization

^{1}H-NMR: ^{1}H NMR was conducted at 9.4 T ($\upsilon_0(^1H)$ = 400.1 MHz) on a BRUKER AVANCE III 400 spectrum equipped with a BBFO probe. ^{1}H chemical shifts were referenced to $CHCl_3$ at 7.28

ppm. ^{1}H NMR spectra was acquired at a spectral width of 12 kHz, a pulse delay of 2 s and 64 scans per spectrum. The NMR samples were prepared by mixing 0.3 mL sample with 0.3 mL $CDCl_3$.

^{2}H-NMR: The ^{2}H NMR experiments were conducted at 9.4 T ($\upsilon 0(^{2}H)$ = 61.4 MHz) on a BRUKER AVANCE III 400 spectrum equipped with a BBFO probe. ^{2}H-NMR spectrums were acquired at a spectral width of 2.5 kHz, a pulse delay of 2 s and 64 scans per spectra.

^{13}C-NMR: The ^{13}C NMR experiments were conducted at 14.1 T ($\nu_0(^{13}C) = 150.9$ MHz) on a BRUKER AVANCE III 600 spectrometer using a zgpg30 pulse program. ^{13}C NMR chemical shifts were referenced to $CDCl_3$ at 77.23 ppm. A spectral width of 36 kHz and a recycle delay of 2 s were used to acquire 10,000 scans per spectrum. The NMR samples in the tubes were prepared by mixing 0.50 mL sample with 0.10 mL $CDCl_3$.

XRD: The powder X-ray Diffraction (XRD) analysis of the catalysts was carried out on a Rigaku ULTIMA III X-ray diffractometer with a Cu Kα irradiation source at a voltage of 40 kV and current of 44 mA. All powder diffraction data were acquired between a 2θ of 3-60º, using 2º step/min.

TGA: Thermographic Analysis (TGA) profiles were used to determine the coke formation and acquired with a simultaneous thermal analyzer (PerkinElmer STA 6000). The samples were held at 30 ºC for 1 min, then heated to 800 ºC at a rate of 20 ºC/min under 30 mL/min air flow.

N_2 Physisorption: N_2 adsorption-desorption analysis of catalysts were carried out on ASAP 2020 Plus surface area and porosimeter system (Micromeritics). The sample was first degassed at 350 ℃ for 4 hours with a temperature ramping rate of 10 ℃ min^{-1} and a vacuum level of 10 mmHg. Then the analysis was performed in liquid nitrogen to get a 56-point adsorption-desorption isotherm. The total surface area was calculated by BET method and the total pore volume was calculated at 0.995 relative pressure.

NH_3-TPD: NH_3-TPD experiments were conducted on the Finesorb-3010 Chemisorption Analyzer. Ammonia was selected as a probe due to its simplicity, small molecular size, and ability to titrate both strong and weak acid sites on the catalyst. Prior to measurements, ~200 mg of fresh sample was calcinated in He flow with 30 sccm at 600 °C for 30 min with a ramp rate of 20 °C/min. The sample was then cooled to 120 °C for adsorption of ammonia, performed using a flow of 25 sccm of 10% NH_3/He for 30 min. After flowing He for 10 min to remove any physically adsorbed NH_3 at 120 ºC, TPD was carried out by ramping to 600 °C with at 10 °C/min and a hold of 30 min under He flow with the rate of 25 sccm. A thermal conductivity detector (TCD) determined the amount of desorbed NH_3. The acquired profiles were fitted and deconvoluted using Bigaussian.

Pyridine absorption: DRIFT spectrum upon pyridine absorption was acquired with a Thermo-Scientific-Nicolet iS50 equipped with an environmental chamber and a liquid-nitrogen cooled mercury–cadmium–telluride (MCT) detector. The gas inlet was connected to a bubbler for pyridine introduction via two three-way valves. Inlet gas (N_2) could pass through the pyridine before entering the chamber. For conducting pyridine adsorption, the fresh catalyst was loaded in the environmental chamber with a 30 sccm N_2 flow for 30 min before collecting background spectra at room temperature (25 ºC). The N_2 flow was then sent into the aforementioned bubbler and carried pyridine vapor into the environmental chamber to conduct pyridine absorption for 20 min. After that, N_2 flow was switched back to bypass the bubbler. The spectrum was recorded in an absorbance mode upon stabilization for 20 min at room temperature.

ICP-OES: The loading amount of metal species on the catalyst is determined on an iCAP 7200 ICP-OES Analyzer (Thermo Fisher Scientific). Samples were first thermally digested for 8 hours in an acid digestion vessel (Parr) using the mixed acids with a volumetric ratio of 1:3:1 for HNO_3, HCl, and HF respectively at a temperature of 463.15 K. Samples were then diluted to an appropriate expected range (1-100 ppm) and analyzed using a PTFE HF resistant introduction system including a Mira Mist nebulizer. After careful calibration, the analysis was conducted with a pump speed of 40 rpm. The exposure time for UV and visible light are 15 and 5 seconds, respectively. The RF power is 1150 W, while the nebulizer gas flow and auxiliary gas flow are 0.55 L/min and 0.5 L/min.

XPS: XPS analysis of the sample was conducted using Kratos Axis spectrometer with monochromatized Al Kα ($h\upsilon$ = 1486.71 eV) radiation. The spectrometer was calibrated by the binding energy (84.0 eV) of Au $4f_{7/2}$ with reference to Fermi level. The pressure of analysis chamber during the experiment was maintained at lower than 5×10^{-10} Torr. The core-level spectra were collected on a hemispherical electron-energy analyzer working at the pass energy of 20 eV, whereas the survey spectrum ranging from 0 to 1200 eV was acquired at analyzer pass energy of 160 eV. The binding energy was calibrated by using C 1s peak at 284.8 eV as a reference. Peak deconvolution of C 1s was conducted using Casa XPS software.

HR-TEM: High Resolution Transmission Electron Microscopy (HR-TEM) was performed on FEI Talos F200X, a high-resolution scanning/ transmission electron microscope (STEM) operated between 80 and 200KV and equipped with HAADF (high angle annular dark field) detector for Z contrast imaging and SuperX EDS detector for compositional analysis.

XANES: XANES measurement was conducted at BL44A of Taiwan Photon Source. The sample was pressed to a pellet with a thickness of 1 mm and placed in the sample holder. The spectrum was acquired in transmission mode. 240 spectra were collected and averaged for each sample. XAFS data analysis was processed following the standard procedure using an IFFEFIT software package. Briefly, in the pre-edge region, the spectrum was fitted to a straight line, and the post-edge background was fitted with a cubic spline. The EXAFS function, χ, was obtained by subtracting the post-edge background from the overall absorption and then normalizing with respect to the edge jump step.

3.4 Bitumen Model Compounds Study

Methylnaphthalene (MN, $C_{11}H_{10}$) was selected as the model compound for investigations on NTP assisted catalytic bitumen partial upgrading. The reactions were conducted by flowing methane, argon and methylnaphthalene in DBD reactor. Total gas flow rate is 60 sccm (30 sccm CH_4 or N_2 + 30 sccm Ar). The methylnaphthalene was flowed into reactor in liquid state with a flow rate of 0.05 ml/min. 3 g catalyst (5%Zn/HY or SiO_2) was loaded in the reactor. The reactor was heated up to 400 ºC.

Cyclohexane (C_6H_{12}), Toluene (C_7H_8), Dodecane ($C_{12}H_{26}$), and Decene ($C_{10}H_{20}$) are chosen as the model compounds to represent naphthenes, monoaromatics, paraffins, and olefins that present in the heavy oil or bitumen. Total gas flow rate is 70 sccm (20 sccm CH_4 + 50 sccm Ar). The gas mixture was flowed through a bubbler filled with liquid reactants. The bubbler was heated up to the temperature that the saturation pressure of liquid reactants is around 0.1 bar. 6 g 5%Zn/HY was loaded in the reactor.

The gas products were analyzed by a four-channel micro-GC (Agilent 490) equipped with a thermal conductivity detector. The first channel equipped with a 10 m molecular sieve 5A

column, which can accurately analyze H_2, O_2, CH_4, and CO. CO_2, C_2H_2, C_2H_4, and C_2H_6 are analyzed in the second channel with a 10 m PPU column. C_3-C_6 and $C_{3=}$-$C_{6=}$ hydrocarbons are determined in the third and fourth channels charged with a 10 m alumina column and an 8 m CP-Sil 5 CB column, respectively. Ar is the carrier gases for the first channel and H_2 is used as the carrier gas for the other three channels. The composition of gas products determined by micro-GC was used to calculate the conversion of gas reactants as well as the yield of gas products based on the ideal gas law. The change of the gas flow rate before and after the reaction was measured using a soap-film flowmeter.

A chiller (-15 ºC) was used to cool the condenser and trap the liquid products. 10 ml of carbon disulfide (99.9%, Sigma-Aldrich) was added to wash the liquid products out from the condenser. The composition of liquid products was analyzed by the pre-calibrated Gas Chromatography-Mass Spectrometer (GC–MS: PerkinElmer GC Claus 680 and MS Clarus SQ 8T) equipped with a Paraffins-Olefins-Naphthenes-Aromatics (PONA) column (Agilent HP-PONA). The oven temperature of GC was set to hold at 40 ºC for 1 min, rise to 110 ºC at 5 ºC /min, ramp to 200 ºC at 10 ºC /min and hold for 5 min. A split ratio of 20 was used for the GC-MS analysis. The mass detector was set to scan the m/z range from 10 to 400. Identification of the compounds was achieved by comparing the mass spectra obtained with those in the system's database (NIST).

The conversion of CH_4 and methylnaphthalene (MN) is defined as:

$$CH_4 \text{ conversion (\%)} = \left(1 - \frac{\text{methane flow rate in gas after reaction}}{\text{methane flow rate in gas fed}} \times 100\right)$$

$$\text{Model compound conversion (\%)} = \left(1 - \frac{\text{mass of model compound in liquid after reaction}}{\text{mass of fed model compound}} \times 100\right)$$

The yield, selectivity and mass balance were calculated based on following equations:

$$\text{Yield (wt. \%)} = \frac{\text{mass of each product}}{\text{mass of fed MN}} \times 100$$

$$\text{Selectivity (C mol\%)} = \frac{\text{mole of carbon in a component in liquid product}}{\text{total moles of carbon in liquid product}} \times 100$$

$$\text{Mass balance (\%)} = \frac{\text{total mass of coke, gas and liquid after reaction}}{\text{total mass of methane and MN before reaction}} \times 100$$

3.5 Plasma-catalytic Conversion of Biogas to Liquid Chemicals

The reaction was performed by flowing methane (99.99%, Praxair) and carbon dioxide (99.9%, Praxair) diluted by Argon (99.999%, Praxair) in DBD reactor. The flow rates of CH_4, CO_2 and Ar are controlled by mass flow controllers and set to be 10, 10, and 50 sccm, respectively.

The conversion of CH_4 and CO_2 is defined as:

$$CH_4 \text{ conversion (\%)} = \frac{\text{moles of } CH_4 \text{ converted}}{\text{moles of } CH_4 \text{ feed}} \times 100$$

$$CO_2 \text{ conversion (\%)} = \frac{\text{moles of } CO_2 \text{ converted}}{\text{moles of } CO_2 \text{ feed}} \times 100$$

The energy efficiency (EE) for the conversion of CH_4 and CO_2 is calculated by:

$$\text{EE (mmol/kJ)} = \frac{\text{moles of } CH_4 \text{ converted (mmol}/min) + \text{moles of } CO_2 \text{ converted (mmol}/min)}{\text{input power (kJ/min)}}$$

The yields of gas (CO, C_xH_y) and liquid products were calculated based on carbon atoms:

$$H_2 \text{ yield } (Y_{H_2}, \%) = \frac{\text{moles of } H_2 \text{ produced}}{2\times\text{moles of } CH_4 \text{ converted}} \times 100$$

$$\text{CO yield } (Y_{CO}, \%) = \frac{\text{moles of CO produced}}{\text{moles of } CH_4 \text{ converted} + \text{moles of } CO_2 \text{ converted}} \times 100$$

$$C_xH_y \text{ yield } (Y_{C_xH_y}, \%) = \frac{\sum_x x\times \text{moles of } C_xH_y \text{ species produced } (x=2,3,4)}{\text{moles of } CH_4 \text{ converted} + \text{moles of } CO_2 \text{ converted}} \times 100$$

The total yield of liquid products (Y_L, %) = 100% - ($Y_{CO} + Y_{C_xH_y}$) - coke determined by TGA.

3.6 Plasma Assisted Natural Gas Utilization

The reactions were performed with methane, propane and argon. Methane with a purity of 99.99 % (provided by Praxair) and propane with a purity of 99.5% (provided by Praxair) were employed as the reactants. Argon with a purity of 99.999% (provided by Praxair) was added into reactant to assist plasma generation. The flow rates of CH_4, C_3H_8 and Ar were 10, 10 and 50 sccm. The flow rates ratio between CH_4 and C_3H_8 may change for reaction condition optimization with a total flow rate of 20 sccm.

Except Ti/UZSM-5 and Ti-Ga/UZSM-5, the preparation method of other catalysts was introduced previously. Ti-Ga/UZSM-5 was prepared via the sol-gel method described by Kanakaraju et al, [102] followed by WI. Typically, certain amount of Titanium (IV) isopropoxide (97%, Sigma-Aldrich) was added dropwise into 100 ml absolute ethanol. The mixture was stirring at 240 rpm for 2 h until the white sol was formed. Then, concentrated HNO_3 was added dropwise until the white precipitate disappeared and a transparent sol formed. The transparent sol was stirring continuously for another 6 h at room temperature to give a transparent yellow sol. UZSM-5 powder was then added into the sol and stirred until a gel was formed. Subsequently, it was oven-dried at 110 °C for 8 h and ground into powder. The prepared Ti/UZSM-5 sample was calcined at 600 °C for 6 h in air. Following the extrusion, certain amount of Ga (1 wt %) was loaded by WI as described above.

To study the effect of UV, the control experiments with external UV source were conducted. 3 UV lamps (Philips, 55 W, 2G11 Base) were evenly installed around the NTP reactor. The distance between the UV lamps and the NTP reactor is around 10 cm. UV lamps is turned on as soon as the reaction starts.

The light emitted from the non-thermal plasma was monitored with a UV/Vis spectrometer (AvaSpec-Uls4096CL-EVO). The slit width of the spectrometer is 10 μm, while the grating was set at 300 lines/mm and the resolution is around 0.6 nm. As presented in **Figure 3**, the spectrum shows a strong peak at 431 nm is in the range of purple light, which is agreed with the color of non-thermal plasma in this study. There also are few peaks at 336, 358 and 388 nm in the range of UVA light and a peak at 309 nm attributed to UVB light. These results confirmed the generation of UV light from the non-thermal plasma.

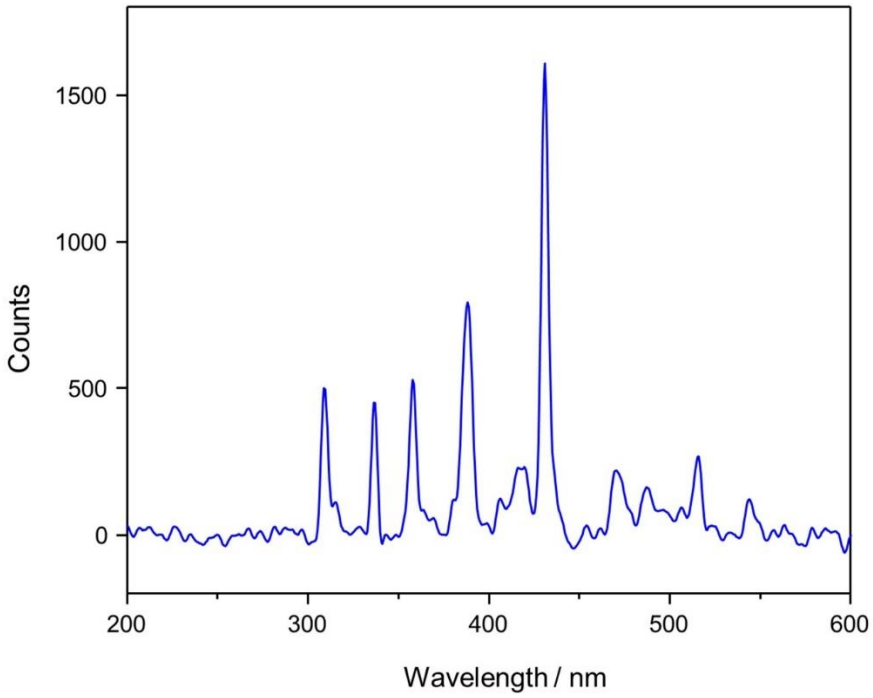

Figure 3. UV/Vis spectrometer spectrum of light emitted from non-thermal plasma

The isotope labelling reactions between propane (99.5%, Praxair) and $^{13}CH_4$ (99.9% ^{13}C, Cambridge Isotope Laboratories, Inc.), CD_4 (99% ^{2}D, Cambridge Isotope Laboratories, Inc.) or CH_4 (99.99 %, Praxair) were conducted in a similar manner when 6 g catalyst was charged. The flow rate of CH_4 (or $^{13}CH_4/CD_4$), C_3H_8 and Ar were 8, 2 and 25 sccm, respectively.

The conversion of methane and propane was calculated by:

$$CH_4 \text{ conversion } (\%) = \left(1 - \frac{\text{moles of } CH_4 \text{ in the gas outlet}}{\text{moles of } CH_4 \text{ in the feed}}\right) \times 100$$

$$C_3H_8 \text{ conversion } (\%) = \left(1 - \frac{\text{moles of } C_3H_8 \text{ in the gas outlet}}{\text{moles of } C_3H_8 \text{ in the feed}}\right) \times 100$$

The yield of hydrogen was defined as:

$$H_2 \text{ Yield } (\%) = \frac{\text{moles of } H_2 \text{ produced}}{2 \times \text{moles of } CH_4 \text{ converted} + 4 \times \text{moles of } C_3H_8 \text{ converted}} \times 100$$

The yield of hydrocarbon in gas products (Y_{gi}) was given by:

$$Y_{gi} \text{ (C \%)} = \frac{i \times \text{moles of } C_i \text{ produced}}{\text{moles of } CH_4 \text{ converted} + 3 \times \text{moles of } C_3H_8 \text{ converted}} \times 100 \ (i = 1 \sim 5)$$

The yield of total gas products (Y_G, C %) was calculated by:

$$Y_G(\text{C \%}) = \sum_{i=1}^{5} Y_{gi}$$

The coke yield (Y_C, C %) was determined by TGA profiles.

The yield of liquid product ((Y_L, C %)) was defined as: $Y_L(\text{C \%}) = 100 - Y_G - Y_C$

The mole concentration of each hydrocarbon in liquid products (y_{li}, mole %) was determined by GC-MS results.

The yield of each hydrocarbon in liquid products (Y_{lj}) was given by:

$$Y_{lj}\ (C\ \%) = Y_L \times \frac{y_{lj} \times j}{\sum_{i=6}^{12} (y_{li} \times i)}$$

The energy efficiency (EE) was defined as:

$$EE\ \left(\frac{mmol}{kJ}\right) = \frac{\text{mmoles of } (CH_4 \text{ converted} + C_3H_8 \text{ converted}) \text{ per second}}{P_{input}\ (W)} \times 1000$$

3.7 Plasma Assisted Liquefied Petroleum Gas Conversion

In a typical run, 6.0 g pelleted catalyst was packed in DBD reactor, and then a mixture of C_3H_8 (99.5%, Praxair), *n*-C_4H_{10} (99.5%, Praxair) with Ar (99.999%, Praxair) were introduced into the reactor. Ar is used as the balanced gas because Ar can facilitate the plasma generation without participation into the reaction. The flow rates of C_3H_8, *n*-C_4H_{10} and Ar were controlled by mass flow controllers and set to be 5, 5, and 40 sccm, respectively. All the experiments were conducted at ca. 9.25 kV peak to peak at load with a constant frequency of 17 kHz at room temperature with 40 min of reaction time. The plasma discharge power was 24-27 W.

Except Ti/UZSM-5 and Ti-Ga/UZSM-5, the preparation method of other catalysts was introduced previously. The catalyst Ti/UZSM-5 was prepared by chemical vapor deposition described by Zhang. [103] 6.0 g pelleted UZSM-5 was put into the quartz reactor and dehydrated in the dry nitrogen at 473 K for 3 h. Then the temperature was set to 873 K. when the temperature stabilized, chemical vapor deposition was initiated by switching Tetrabutyltitanate (Sigma-Aldrich, 97%, TBOT) as Ti precursor with a carrier gas flow rate of 200 ml/min and the precursor temperature was 333 K. TBOT was transported into the reactor where it decomposed and TiO_2 particles formed. After 3 h of deposition at 873 K, the reactor was purged by nitrogen gas for 1 h. The Ti-Ga/UZSM-5 was prepared by chemical vapor deposition described above using pelleted Ga/UZSM-5 as the starting material.

The conversion of light hydrocarbon (C_nH_{2n+2}, n=1, 2, 3, 4) was calculated by:

$$C_nH_{2n+2}\ \text{conversion}\ (\%) = \frac{\text{moles of } C_nH_{2n+2} \text{ converted}}{\text{moles of } C_nH_{2n+2} \text{ fed}} \times 100$$

The yield of hydrocarbons (C_i) in gas products (Y_i) was given by:

$$Y_i\ (C\ \%) = \frac{i \times \text{moles of } C_i \text{ produced}}{\sum_{n=1}^{4} n \times \text{moles of } C_nH_{2n+2} \text{ converted}} \times 100\ (i = 1, 2, 3, 4, 5)$$

The yield of total gas products (Y_G, C %) was calculated by:

$$Y_G(C\ \%) = \sum_{i=1}^{5} Y_i$$

The coke yield (Y_C, C %) was determined by TGA profiles, in which the coke was calculated by weight loss from 300 to 700 °C assuming coke is composed of pure carbon.

The yield of liquid product (Y_L, C %) was defined as: $Y_L(C\ \%) = 100 - Y_G - Y_C$

4 RESULTS AND DISCUSSION

4.1 Bitumen Model Compound Study

4.1.1 NTP assisted catalytic upgrading of MN under methane

The results shown in **Table 1** indicate that methane could slightly improve MN conversion and the yield of monoaromatics, while plasma presence could favor methane conversion, MN conversion, and the yield of monoaromatics. The catalyst with acidity could significantly promote MN conversion and the formation of monoaromatics, however, leading to severe coke formation. Decreasing the flow rate of MN could benefit the formation of monoaromatics with less coke. Higher selectivity of monoaromatics is observed when using HZSM5 catalyst instead of HY, probably due to the shape selectivity.

Table 1. Performance of NTP catalytic upgrading of MN under various reaction conditions

Reaction conditions	Catalyst	5%Zn/HY	5%Zn/HY	5%Zn/HY	SiO_2	5%Zn/HY	5%Zn/HY	5%Zn/HZSM-5
	WHSV (h^{-1})	1	1	1	1	0.6	0.5	1
	Plasma	On	On	Off	On	On	On	On
CH_4 conversion (%)		4.6	N/A	0.1	0.4	4.6	5.1	1.1
MN conversion (%)		61.3	57.9	49.4	1.7	61.3	68.9	71.7
Mass balance (%)		102.8	100.7	98.3	100.6	102.8	97.7	99.4
		Yield (wt.%)						
Gas		0.8	0.8	0.3	0.1	1.7	1.6	1.0
Coke		25.5	24.8	17.7	0.4	17.9	36.6	2.4
Liquid		79.6	77.5	79.8	100.6	76.4	60.6	92.2
		Liquid Product Selectivity (C %)						
Mono aromatics		0.4	0.2	0.3	2.8	1.8	0.7	2.9
Naphthalene		49.6	58.8	43.6	38.1	39.1	55.1	36.4
Alkyl naphthalene		50.0	41.0	56.1	59.1	59.1	44.2	60.7

4.1.2 NTP assisted catalytic upgrading of other heavy oil model compound

Cyclohexane (C_6H_{12}), Toluene (C_7H_8), Dodecane ($C_{12}H_{26}$), and Decene ($C_{10}H_{20}$) are chosen as the model compounds to represent naphthenes, monoaromatics, paraffins, and olefins that present in the heavy oil. The results listed in **Table 2** suggest that the ring including cycloalkane ring and aromatic ring is difficult to be opened under NTP conditions, and the major reaction is ring alkylation for the conversion of cyclohexane or toluene while cracking, C-C coupling, and hydrogenation are the dominant reactions for the conversion of dodecane or decene.

Table 2. Plasma-catalytic conversion of heavy oil model compounds

Model Compound (MC)	Cyclohexane	Toluene	Dodecane	Decene
CH_4 conversion (%)	4.6	8.3	27.7	27.5
MC conversion (%)	61.3	12.1	5.9	100
	Yield (C %)			
Gas	19.3	10.1	45.3	30.9
Liquid	57.2	6.7	40.6	60.6
Coke	26.7	87.9	23.8	16.6
	Reaction Selectivity (based on liquid product) (C %)			
Ring opening	1	0	0	0
Ring extension	7	34	0	0
Isomerization	9	0	13	0
Demethylation	0	16	0	0

Cracking	0	0	55	65
C-C coupling	83	44	32	17
Hydrogenation	0	6	0	18

4.1.3 Conclusion

The investigations of various model compounds show that NTP technology may not apply to directly upgrading of heavy oil with high boiling point, because NTP technology is quite effective for gas phase reaction but much less effective for liquid phase reaction. Interestingly, the complete conversion of olefin is achieved at atmospheric pressure and low temperature under the facilitation of NTP, which could be potentially used for olefin reduction of bitumen. It is observed that the obtained liquid products contain much more isomeric paraffins than olefins, and NTP reaction favors carbon chain extension *via* C-C coupling when using light hydrocarbons (C_1-C_4) as the reactant.

4.2 Plasma-catalytic Conversion of Biogas to Liquid Chemicals

Biogas is a promising renewable energy source consisting of methane (55-65%) and carbon dioxide (35-45%) produced from the anaerobic digestion of biomass, landfill, and wastewater treatment. The results in **Table 3** show that the formation of liquid products is observed when packing a catalyst with acidity under NTP mode. When combining NTP and UZSM-5 catalyst, the conversion of CH_4 and CO_2 is 23.9 % and 13.7 %, respectively, and 59 % yield of liquid products with limited carbon deposition (5.1%) is achieved. H_2 and CO are the major gas products detected by micro GC, and the collected liquid products are C_1-C_3 oxygenates including formaldehyde (HCHO), methanol (CH_3OH), ethanol (C_2H_5OH), and acetone (CH_3COCH_3) as confirmed by GC-MS and ^{1}H NMR in **Figure 3**. The reforming of biogas to liquid chemicals in the presence of a plasma is likely to occur *via* radical chain mechanism, where, CO, CH_3, and OH radicals are considered to be the key species during the plasma-catalytic CH_4/CO_2 conversion. [104] In a plasma environment, the gas reactant is vibrationally and electronically excited by electron impact reactions and dissociated into CO and O radicals. The electron impact dissociation of CH_4 and CO_2 generates H, CO, O, OH and CH_x (x=1-3). The recombination of radical forms gas and liquid products. The alteration in plasma discharge behavior by placing the catalyst in DBD, which has been characterized as a shift from gas microdischarges to surface discharges and weaker microdischarges,[105] may effectively inhibit the direct dissociation of CH_x to form carbonaceous species.

Moreover, the porous structure of the catalyst could offer higher specific surface area for the radical reactions, thus enhancing liquid yield.

Table 3. The effect of operating modes and various support on the plasma-catalytic conversion of biogas

	Catalyst only	Plasma only	Plasma + Catalyst			
			CZSM-5	γ-Al_2O_3	SiO_2	UZSM-5
CH_4	0	25.4	24.2	19.4	17.0	23.9
CO_2	0	14.7	15.3	10.7	10.9	13.7
H_2 yield	0	40.8	38.9	50.3	49.4	38.4
	Yield (C %)					
CO	0.0	22.9	18.4	21.1	26.5	20.5
C_xH_y	0.0	19.4	12.3	21.2	24.5	15.7

Liquid	0.0	0.0	34.4	25.8	0.0	59.0
Coke	0.0	57.7	34.9	31.9	49.0	5.1

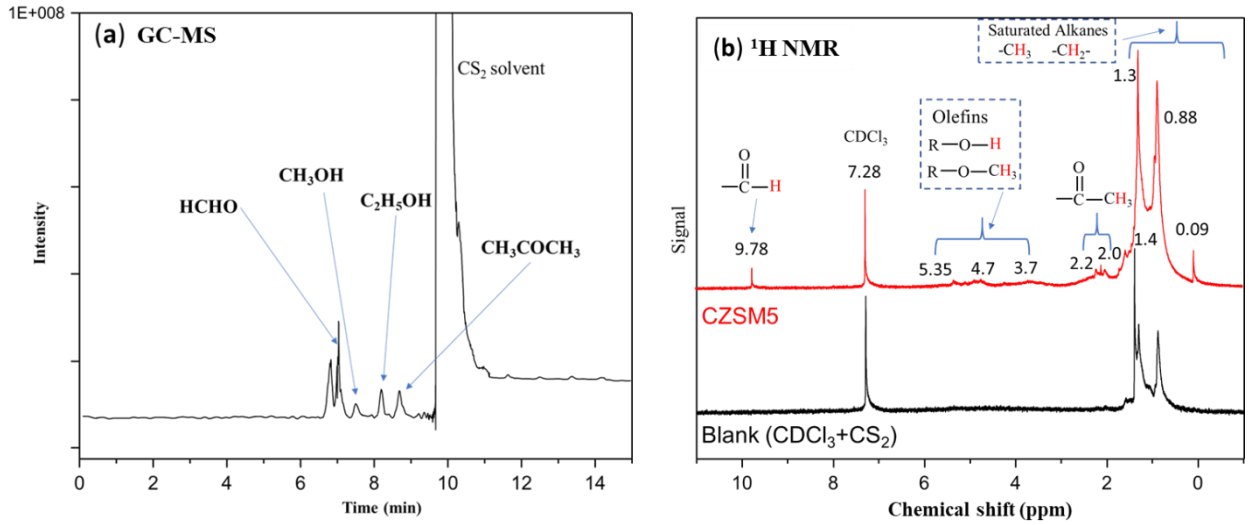

Figure 4. GC-MS(a) and ^{1}H NMR (b) analyses of the liquid products

Modification of supports (CZSM-5 and UZSM-5) with metal species (Ag, Pt, Pd, Re, and Ir) is conducted to further improve the liquid yield. Based on the results (not shown), the addition of Ag, Re or Ir on CZSM-5 decreases the conversion of CH_4 and CO_2, and slightly enhances the gas yield. However, there is little effect on the formation of liquid products and coke reduction. Pd loading on CZSM-5 results in higher yield of gas products (especially, CO yield increased by 9.3%) and lower coke formation (reduced by 18.6%) but has limited promotion effect on the liquid yield (increased by 5.5%). The highest liquid yield (60.7%) with the lowest coke formation (9.3%) is achieved when Pt is introduced on CZSM-5, and the coke formation is further reduced to 5.1 % when Pt is loaded on UZSM-5. Therefore, Pt/UZSM-5 shows the best plasma-catalytic performance among these catalysts.

Acidity characterization with NH_3-TPD (not shown) suggest that the number of acidic sites may be not a determining factor for the reaction performance. The acidity feature has little effect on the conversion of CH_4 and CO_2, probably due to both are exclusively plasma-activated at such a low reaction temperature. However, the acidity feature greatly affects the formation of liquid and coke products. No acidic site (SiO_2) or higher ratio of medium and/or strong acidic sites (>30%, e.g. γ-Al_2O_3, CZSM-5, Ag/CZSM-5, Re/CZSM5) would lead to more coke formation (30~50%) with 25~35% of liquid yield. Less coke (<20%) and more liquid products (40~60%) are observed over the catalysts with higher ratio of weak acidic sites (>70%, e.g. Pt/CZSM-5, Pd/CZSM-5). The presence of acidic sites is necessary, which could promote the stabilization of the oxygenated intermediates (e.g. CO, CH_3CO radicals) to form more liquid products. However, the strong interaction between strong/medium acidic sites and the intermediates could trap the formed products on the catalyst surface, suffering further attack from the plasma to form carbonaceous species as the final products. Pt loading on UZSM-5 leads to the disappearance of medium acidic sites of UZSM-5, which further reduces the coke formation to 5.1% and increases the liquid yield by 7.8%. Therefore, higher ratio of weak acidic sites and Pt active sites benefit the formation of active carbonaceous species, thus reduces the coke formation.

In summary, our work demonstrates the direct plasma-catalytic conversion of biogas to valuable liquid chemicals with limited coke formation at low temperature and ambient pressure. Combining NTP with the catalyst enhances the formation of liquid products whilst significantly inhibiting coke formation. High liquid yield with low carbon deposition is achieved over a unique Pt/UZSM5 catalyst. The total yield of liquid chemicals reaches approximately 60%, with the composition of formaldehyde, methanol, ethanol, and acetone. Coke formation is limited to 5.1%. The liquid yield and coke formation can be controlled by the modification of acidic properties and Pt species. High ratio of weak acidic sites benefits the formation of liquid chemicals and coke reduction. These findings suggest that the combination of NTP and heterogeneous catalysis has the great potential to produce renewable oxygenates from the biogas conversion with limited carbon deposition. This work is published on the journal of Energy Conversion and Management.

4.3 Plasma Assisted Natural Gas Utilization

Natural gas is an abundant, cheap and underutilized natural resource with increasing proved reserves as well as an agricultural by-product. A simulated natural gas, methane and propane, is used to investigate the feasibility of the conversion of natural gas into valuable liquid chemicals via NTP technology. NTP catalytic conversion of methane and propane produces various C_6-C_9 alkane compounds as the liquid products, H_2, C_2H_6, and C_3H_6 as the major gas products with a small amount of C_2H_4, C_2H_2, C_4-C_5 hydrocarbons, and coke. Moreover, GC-MS analysis also shows that the liquid products consists of C_6-C_9 alkanes with a predominantly branched structure, which could be potentially used as gasoline or high-value aviation fuel for aircrafts.[106]

The reaction performance suggests that similar conversion of methane or propane are observed over different supports (SiO_2, γ-Al_2O_3, HZSM-5, UZSM-5) and supported various metal (Ag, Ga, Pd, Pt) modified UZSM-5 catalysts. This is understandable because methane and propane are exclusively activated by plasma at such low reaction temperature. It is worth noting that methane conversion (1.3-4.1%) is much lower than propane conversion (26.9- 36.4%), which is attributed to the higher bond dissociation energy of C-H in methane (439.3 kJ/mol), compared to that of C-H (422.2 kJ/mol, 410.5 kJ/mol) or C-C (370.3 kJ/mol) in propane.[107] However, the product distribution varies heavily depending on the charged support. There is no detectable liquid product over SiO_2 or γ-Al_2O_3, while more than 30 C% yield of liquid products is obtained over bare zeolite such as HZSM-5, UZSM-5. This result suggests that the support's acidity and morphology may be critical for the formation of hydrocarbons with high carbon number (C_6-C_9). Moreover, the coke yield is significantly reduced over HZSM-5 (30.7 C%), compare to that over SiO_2 (44.1 C%) or γ-Al_2O_3 (50.2 C%). Coke formation is further inhibited over UZSM-5 (9.7 C% coke yield) with uniform cylindrical shape. Coke formation can be further suppressed by modification with metal species (Ag, Ga, Pd, Pt). Compared to UZSM-5, the addition of Ga addition reduces the yield of both coke and gas products, thus, promotes the formation of liquid products (increased by 10.5 C%). Ga/UZSM-5 is thus selected as the preferred catalyst for further investigations. Ultraviolet radiation can be self-generated by non-thermal dielectric barrier discharge plasma,[108] which drives us to integrate plasma activation and photocatalysis for natural gas conversion. Ga/UZSM-5 modification with TiO_2 (a widely used as the photocatalyst material) is synthesized as the photocatalyst to further enhance the performance on the conversion of simulated natural gas. Compared to Ga/UZSM-5, methane conversion and coke yield over Ti-Ga/UZSM-5 are quite similar, however, higher propane conversion (increased by 11.2 %) and more C_6-C_9 hydrocarbons (the yield boosted from 37.9 C% to 58.4 C%) are

obtained. A plausible explanation could be that the photocatalyst Ti-Ga/UZSM-5 notably enhances the energy utilization efficiency through incorporation of the energy present in the co-existing UV/visible light formed during plasma generation. In other words, more input energy is utilized for reactants conversion, particularly for propane conversion since propane is much easier to be activated compared to methane due to the aforementioned lower molecular activation energy. Higher propane conversion would provide more C_1-C_3 radicals for the formation of C_6-C_9 hydrocarbons. As a result, more liquid products are formed over Ti-Ga/UZSM-5.

The roles of plasma and a catalyst played in the co-conversion of methane and propane are verified by conducting equivalent reactions with/without plasma or a catalyst. As shown in **Table 4**, it is expected that there is no reaction without plasma as evidenced by no conversion of methane or propane in the catalyst only mode. When plasma is applied, approximately 0.125 mmol methane and/or propane molecules per kilojoules are converted regardless of the catalyst under stable conditions. This supports the previous hypothesis that methane and propane are exclusively activated by plasma. For the test without a catalyst, SiO_2 is placed in the reactor as the inert material to reduce the effect of mass or heat transfer on the reaction. No liquid products collected in the plasma-only mode implies that the catalyst with an appropriate acidity is essential for C-C coupling reaction to form hydrocarbons with longer chain or more branches. The presence of propane in methane offers more C_1-C_3 radicals to terminate the further cleavage of methyl radicals from methane, therefore, more branched hydrocarbons are formed as evidenced by a higher yield of C_7-C_8 hydrocarbons with less coke.

Isotope labeled CH_4 ($^{13}CH_4$ and CD_4) is employed to elucidate the evolution of C and H of methane in the reaction. As shown in **Figure 5**, compared to ^{13}C signal from the non-isotopic labeled counterpart (CH_4 + C_3H_8), ^{13}C signal acquired from the $^{13}CH_4$ run ($^{13}CH_4$ + C_3H_8) is significantly enhanced (the peak area with respect to $CDCl_3$ reference increases from 0.3 to 11.0), which strongly supports methane incorporation into the final products. This is highly consistent with the observation in ^2H-NMR spectra as shown in **Figure 5b**, where there is a broad deuterium peak (0- 2 ppm) which can be deconvoluted into 3 peaks at 0.9, 1.3, and 1.6 ppm, corresponding to $-CD_3$, $-CD_2$ and -CD, respectively.

Table 4. The reaction performance of methane and propane conversion over different reaction conditions

Reaction Condition		$CH_4 + C_3H_8$ [a]	Pure CH_4 [b]	Pure C_3H_8 [c]	Catalyst only[d]	Plasma only [e]
Conversion (%)	CH_4	3.3	23.7	0.0	0.0	2.4
	C_3H_8	36.4	0.0	23.5	0.0	34.6
Yield of H_2 (%)		23.6	48.1	19.2	0.0	25.1
Gas product yield (C %)	C_1	0.0	0.0	10.3	0.0	0.0
	C_2	25.9	51.9	28.8	0.0	24.4
	C_3	13.7	17.1	16.7	0.0	16.7
	C_4	8.4	4.8	7.4	0.0	11.0
	C_5	3.2	1.4	3.9	0.0	3.8
	Sum	51.3	75.3	67.1	0.0	55.9
Liquid product yield (C %)	C_6	15.9	0.7	15.1	0.0	0.0
	C_7	15.3	1.9	8.5	0.0	0.0
	C_8	10.2	0.9	6.0	0.0	0.0
	C_9	2.6	0.0	2.3	0.0	0.0

	$\geq C_{10}$	0.0	0.0	0.0	0.0	0.0
	Sum	43.4	3.5	28.9	0.0	0.0
Coke yield (C %)		5.3	21.2	4.1	0.00	44.1
EE (mmol/kJ)		0.115	0.139	0.137	0.00	0.108

(Reaction conditions: 50 sccm Ar as the carrier gas, discharge power 24-27 W, catalyst or SiO_2 *ca.* 6 g; a: 10 sccm CH_4, 10 sccm C_3H_8, plasma, Ga/UZSM-5; b: 20 sccm CH_4, plasma, Ga/UZSM-5; c: 20 sccm C_3H_8, plasma, Ga/UZSM-5; d: 10 sccm CH_4, 10 sccm C_3H_8, no plasma, Ga/UZSM-5; e: 10 sccm CH_4, 10 sccm C_3H_8, plasma, SiO_2.)

This study highlights the synergy of plasma activation and photocatalysis in the upgrading of simulated natural gas. We demonstrate an efficient protocol for non-thermal plasma assisted photo-catalytic conversion of natural gas, which is cheap, abundant and naturally available, to gasoline range chemicals at ambient conditions, thus greatly reducing the heavy dependence on finite other fossil fuels such as oil and coal. The herein formed liquid chemicals are C_6-C_9 alkanes with predominantly isomeric structures, which could be potentially used for high-value aviation fuel. Over 58.4 C% total yield of gasoline products with limited coke formation (6.3 C%) can be achieved by coupling plasma and photocatalysis. The results from isotope labeling experiments clearly show that methane tends to be incorporated into 1-C or 2-C of formed alkane as a terminal group. To conclude, this work offers the opportunities of merging non-thermal plasma and photocatalysis, providing an environmentally superior option to meet rapidly growing energy demands.

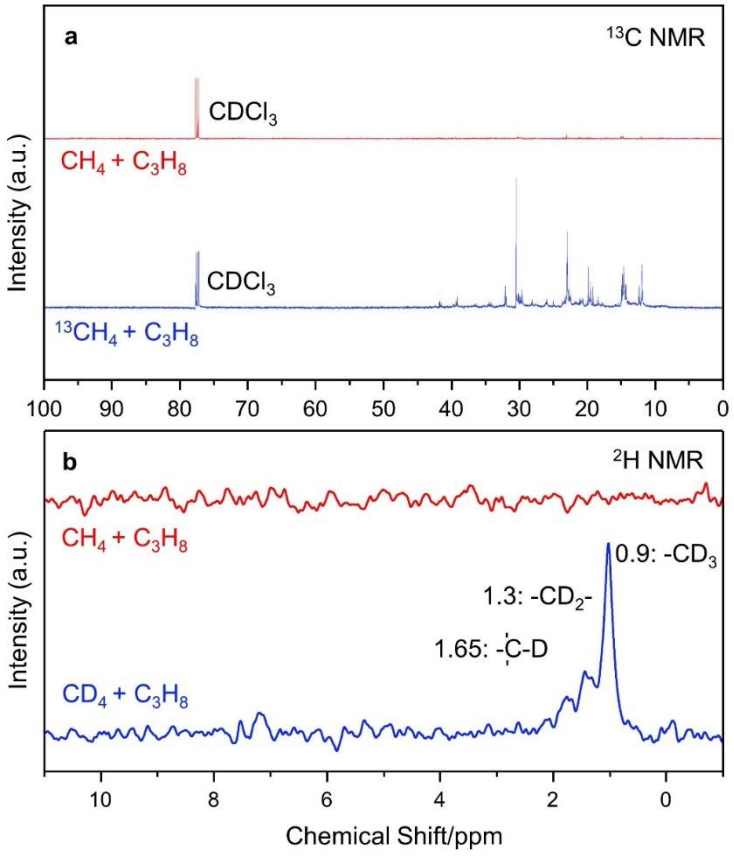

Figure 5. Isotope labeling investigations on the conversion of methane and propane.

4.4 Plasma Assisted Liquefied Petroleum Gas Conversion

Liquefied petroleum gas (LPG) is a cheap resource that is mainly used as fuel in heating appliances, cooking equipment, and vehicles. GC-MS analysis shows that NTP reaction with LPG generates C_6-C_{10} iso-alkanes as the major liquid products, and H_2, methane and C_2 hydrocarbons as the main gas products. It is observed from the experimental results (**Table 5**) that the conversion of propane is higher than that of butane. One explanation could be due to the recombination of C_2 radicals to form butane which decreases the conversion of butane. More gas products over SiO_2 suggest that packing catalyst and acidity could be beneficial for the formation of liquid products. Less coke formation is obtained over UZSM-5, however, more gas products is produced. More importantly, the liquid products over UZSM-5 exclusively contain C_6-C_8 alkanes with a small number of olefins. The distribution of liquid products over three metal (Ga, Pt, Ti) modified catalysts is similar, which shows high selectivity of C_6-C_9 iso-alkanes. However, higher yield of liquid products is obtained over Ga/UZSM-5, while lower yield is observed over Pt/UZSM-5 and Ti/UZSM-5. Theoretically, more methane and C_2 hydrocarbons will results in less H_2 yield, and more liquid products (>=C_6) or coke will generate more H_2. Ga introducing may convert more C_2 hydrocarbon to liquid products, thus producing more liquid products. Pt or Ti loading generates more C_2 hydrocarbons with less H_2, thus leading to less liquid products. When co-loading Ga and Ti on UZSM-5, it is observed that the conversions of both propane and butane increase and the liquid yield is also improved. This is due to higher energy utilization efficiency by Ti addition which could absorb the UV/visible light generated by DBD plasma, therefore, the co-loading of Ga and Ti could further decrease the formation of C_2 gas species, thus resulting in more liquid products.

Table 5. Non-thermal plasma catalytic performance on the conversion of propane and butane to liquid chemicals over various catalysts

Catalyst		SiO_2	HZSM-5	UZSM-5	Ga/UZSM-5	Pt/UZSM-5	Ti/ UZSM-5	Ti-Ga/ UZSM-5
Conv. (%)	C_3H_8	27.3	28.7	28.1	27.9	28.3	28.1	33.3
	n-C_4H_{10}	9.2	8.9	9.2	9.3	9.5	8.3	10.1
		The yield of products (C %)						
Gas	CH_4	15.1	14.5	15.1	16.0	17.3	15.8	9.6
	C_2H_6, C_2H_4	51.1	25.9	44.3	34.5	48.7	47.4	32.9
	n-C_5H_{12}	3.8	6.0	4.6	4.6	4.5	5.6	4.2
	Sum	70.0	46.5	64.1	55.1	70.4	68.8	46.7
Liquid		6.8	18.9	26.2	39.8	23.9	20.0	47.8
Coke		23.2	34.6	9.8	5.1	5.7	11.2	5.5
		The composition of liquid product (C %)						
C_6		N/A	28.5	25.8	34.5	25.2	33.1	40.2
C_7		N/A	27.2	38.8	41.8	37.3	39.7	37.5
C_8		N/A	18.0	25.0	18.6	21.1	21.7	18.1
C_9		N/A	10.0	10.4	5.1	7.5	5.5	4.2
≥C_{10}		N/A	16.3	0.0	0.0	8.9	0.0	0.0

(Reaction conditions: 50 sccm of gas mixture (10% C_3H_8, 10% n-C_4H_{10}, 80% Ar), 40 min, discharge power 24-27 W, ca. 6 g catalyst.)

5 CONCLUSIONS AND RECOMMENDATIONS

5.1 Conclusions

Most of the original objectives in the proposal have been reached by the end of this project. Catalytic assisted DBD reactor has been developed and tested for both gas and gas-liquid reactions, and optimal conditions for safe plasma generation has been established. The investigations on various model compounds including MN, cyclohexane, toluene and indicate that both cycloalkane and aromatic rings are difficult to open, and ring alkylation is the major reaction under the plasma conditions. The reactions with dodecane and decene imply that cracking, C-C coupling, and hydrogenation are the dominant reactions. Our observations suggest liquid substrate is hardly activated by plasma, and NTP technology is very effective for gas phase reaction, carbon chain extension, and olefin reduction. More research effort has been focused on the gas phase reaction, such as the conversion of light hydrocarbons (biogas, natural gas, LPG) to valuable liquid chemicals. One unique photocatalyst Ti-Ga/UZSM5 are developed. This catalyst could utilize the UV/Visible light generated from plasma, thus significantly increase the conversion, improve the liquid yield, and control the coke formation.

The achievements of this project demonstrate that NTP technology is effective for hydrogenation of double bond (C=C) and carbon chain extension by C-C coupling. Biogas (CH_4 and CO_2) is primarily used to produce syngas via dry reforming reaction, and light hydrocarbons (C_1-C_4) are mainly used as a source of energy for residential heating, cooking, and power generation. Under the facilitate of NTP technology, biogas can be converted to more valuable liquid chemicals such as formaldehyde, methanol, ethanol, and acetone rather than syngas; light hydrocarbons such as natural gas and LPG can be transformed to C_6-C_9 branched-chain alkanes at low temperature and atmospheric pressure. More importantly, coke formation is well controlled by incorporating a catalyst unique photocatalyst, and coke yield is much lower than that has been previously reported by other researchers. The coupling plasma and photocatalysis could significantly improve the conversion of the reactant and the yield of liquid products. The investigations on reaction mechanism using isotope labeling molecules clearly show that methane tends to be incorporated into 1-C or 2-C of alkane as a terminal group. These findings provide an environmentally superior option to meet rapidly growing energy demands.

NTP technology shows great potential to produce high-quality gasoline range chemicals from light paraffins (C_1-C_4), which can be achieved in one step. From the viewpoint of engineering practice, one pot process developed in this project has the potential to make the utilization of natural gas more economically profitable.

5.2 Recommendations for Future Work

The current outcomes show promising results in gasoline range chemicals production from light paraffins. However, further optimization of reactor configuration and reaction parameters are suggested for increased energy efficiency. Catalyst screening will be conducted with a sulfur-containing mixture or using pre-sulfided catalysts for short-term experiments. Best practice is presulfiding plus a low concentration of H_2S mixed with the feed. This approach avoids the problem of transient metal phases in the catalyst as reactions with sulfur occur. To optimize the catalyst design and gain a better understanding of reaction mechanism, the quantum molecular calculation and molecular dynamic simulation will be performed.

Once a proof of concept has been determined form a chemistry perspective, then the reactor design will be re-visited from a strictly chemical engineering approach. Several kinetic models

will be proposed to simulate the mechanistic behavior of the plasma-catalyst system. If the estimated values are well consistent with the experimental results, the hypothesized reaction pathways and rate-determining step will uncover the actual reaction mechanism to a certain level. The outcomes from the kinetic analysis will benefit the reactor design. In addition to the control experiments to prove the synergistic benefit, other techniques, such as isotopic labeling technique (i.e. CD_4 or $^{13}CH_4$), TOF-SIMS, NMR and/or MS will be employed to understand the underlying mechanism, which is very crucial to rationally design catalyst structure for achieving enhanced performance. The evaluation of economic feasibility is also very important for further industrial application.

6 ACKNOWLEDGEMENTS

We gratefully acknowledge the financial supports from Natural Sciences and Engineering Research Council of Canada (NSERC) through collaborative research and development program (CRDPJ/506994-2016) and Institute for Oil Sands Innovation at University of Alberta (IOSI 2016-06).

7 REFERENCES

1. Belyk, G.; Burgart, D.; Jablonski, B.; Heida, J.; Kaiser, T.; Bernar, R.; Whitelaw, B. J. P. H., Canadian Heavy Oil Association, Heavy Oil 101. **2013**.

2. Mech, M. J. U. t. e.; human impacts, e. i.; political, e.; industry implications; political, e.; Canada, i. i. G. p. o., A comprehensive guide to the Alberta oil sands. **2011**.

3. Furimsky, E., *Catalysts for upgrading heavy petroleum feeds*. Elsevier: 2007.

4. Ovalles, C.; Hamana, A.; Bolivar, R.; Morales, A., Process for treating heavy crude oil. Google Patents: 1993.

5. Ovalles, C.; Filgueiras, E.; Morales, A.; Scott, C. E.; Gonzalez-Gimenez, F.; Embaid, B. P. J. F., Use of a dispersed iron catalyst for upgrading extra-heavy crude oil using methane as source of hydrogen☆. **2003,** *82* (8), 887-892.

6. Ovalles, C.; Filgueiras, E.; Morales, A.; Rojas, I.; de Jesus, J. C.; Berrios, I. J. E.; fuels, Use of a dispersed molybdenum catalyst and mechanistic studies for upgrading extra-heavy crude oil using methane as source of hydrogen. **1998,** *12* (2), 379-385.

7. Bhasin, G. E. K. a. M. M., Synthesis of ethylene via oxidative coupling of methane: I. Determination of active catalysts. *Journal of Catalysis* **1982,** *73* (1), 9-19.

8. Ito, T., Wang, J., Lin, C. H., and Lunsford, J. H. , Oxidative dimerization of methane over a lithium-promoted magnesium oxide catalyst. *Journal of the American Chemical Society* **1985,** *107* (18), 5062-5068.

9. Wang, L., Tao, L., Xie, M., Xu, G., Huang, J., and Xu, Y. , Dehydrogenation and aromatization of methane under non-oxidizing conditions. *Catalysis Letters* **1993,** *21* (1-2), 35-41.

10. Guo, X., Fang, G., Li, G., Ma, H., Fan, H., Yu, L., ... and Tan, D., Direct, nonoxidative conversion of methane to ethylene, aromatics, and hydrogen. *Science* **2014,** *344* (6184), 616-619.

11. Ashcroft, A. T., Cheetham, A. K., and Green, M. , Partial oxidation of methane to synthesis gas using carbon dioxide. *Nature* **1991,** *352* (6332), 225-226.

12. Rostrupnielsen, J. R., and Hansen, J. B., CO2-reforming of methane over transition metals. . *Journal of Catalysis* **1993,** *144* (1), 38-49.

13. Lee, J. S.; Oyama, S. J. C. R. S.; Engineering, Oxidative coupling of methane to higher hydrocarbons. **1988,** *30* (2), 249-280.

14. Lunsford, J. H. J. A. C. I. E. i. E., The catalytic oxidative coupling of methane. **1995,** *34* (9), 970-980.

15. Hutchings, G.; Scurrell, M.; Woodhouse, J. J. C. S. R., Oxidative coupling of methane using oxide catalysts. **1989,** *18*, 251-283.

16. Amenomiya, Y.; Birss, V. I.; Goledzinowski, M.; Galuszka, J.; Sanger, A. R. J. C. R. S.; Engineering, Conversion of methane by oxidative coupling. **1990,** *32* (3), 163-227.

17. Sahebdelfar, S.; Ravanchi, M. T.; Gharibi, M.; Hamidzadeh, M. J. J. o. n. g. c., Rule of 100: An inherent limitation or performance measure in oxidative coupling of methane? **2012,** *21* (3), 308-313.

18. Kolyagin, Y. G.; Ivanova, I. I.; Ordomsky, V. V.; Gedeon, A.; Pirogov, Y. A. J. T. J. o. P. C. C., Methane Activation over Zn-Modified MFI Zeolite: NMR Evidence for Zn− Methyl Surface Species Formation. **2008,** *112* (50), 20065-20069.

19. Guczi, L.; Koppány, Z.; Sarma, K.; Borkó, L.; Kiricsi, I., Structure and catalytic activity of Co-based bimetallic systems in NaY zeolite: low temperature methane activation. In *Studies in Surface Science and Catalysis*, Elsevier: 1997; Vol. 105, pp 861-868.

20. Xu, Y.; Lin, L. J. A. C. A. G., Recent advances in methane dehydro-aromatization over transition metal ion-modified zeolite catalysts under non-oxidative conditions. **1999,** *188* (1-2), 53-67.

21. Xu, Y.; Bao, X.; Lin, L. J. J. o. C., Direct conversion of methane under nonoxidative conditions. **2003,** *216* (1-2), 386-395.

22. Cui, Y.; Xu, Y.; Lu, J.; Suzuki, Y.; Zhang, Z.-G. J. A. C. A. G., The effect of zeolite particle size on the activity of Mo/HZSM-5 in non-oxidative methane dehydroaromatization. **2011,** *393* (1-2), 348-358.

23. Alvarez-Galvan, M.; Mota, N.; Ojeda, M.; Rojas, S.; Navarro, R.; Fierro, J. J. C. t., Direct methane conversion routes to chemicals and fuels. **2011,** *171* (1), 15-23.

24. Ha, V. T. T.; Sarıoğlan, A.; Erdem-Şenatalar, A.; Taârit, Y. B. J. J. o. M. C. A. C., An EPR and NMR study on Mo/HZSM-5 catalysts for the aromatization of methane: Investigation of the location of the pentavalent molybdenum. **2013,** *378*, 279-284.

25. Choudhary, T. V.; Aksoylu, E.; Wayne Goodman, D. J. C. r., Nonoxidative activation of methane. **2003,** *45* (1), 151-203.

26. Choudhary, V. R.; Kinage, A. K.; Choudhary, T. V. J. S., Low-temperature nonoxidative activation of methane over H-galloaluminosilicate (MFI) zeolite. **1997,** *275* (5304), 1286-1288.

27. Baba, T.; Sawada, H. J. P. C. C. P., Conversion of methane into higher hydrocarbons in the presence of ethylene over H-ZSM-5 loaded with silver cations. **2002,** *4* (15), 3919-3923.

28. Anunziata, O. A.; Cussa, J.; Beltramone, A. R. J. C. t., Simultaneous optimization of methane conversion and aromatic yields by catalytic activation with ethane over Zn-ZSM-11 zeolite: The influence of the Zn-loading factor. **2011,** *171* (1), 36-42.

29. Choudhary, V. R.; Mondal, K. C.; Mulla, S. A. J. A. C., Simultaneous Conversion of Methane and Methanol into Gasoline over Bifunctional Ga‐, Zn‐, In‐, and/or Mo‐Modified ZSM‐5 Zeolites. **2005,** *117* (28), 4455-4459.

30. Gray, M. R., *Upgrading oilsands bitumen and heavy oil*. University of Alberta: 2015.

31. Guo, A.; Wu, C.; He, P.; Luan, Y.; Zhao, L.; Shan, W.; Cheng, W.; Song, H. J. C. S.; Technology, Low-temperature and low-pressure non-oxidative activation of methane for upgrading heavy oil. **2016,** *6* (4), 1201-1213.

32. Zhao, L.; He, P.; Jarvis, J.; Song, H. J. E.; Fuels, Catalytic Bitumen Partial Upgrading under Methane Environment over Ag-Mo-Ce/ZSM-5 Catalyst and Mechanistic Study Using N-Butylbenzene as Model Compound. **2016,** *30* (12), 10330-10340.

33. He, P.; Luan, Y.; Zhao, L.; Cheng, W.; Wu, C.; Chen, S.; Song, H. J. F. P. T., Catalytic bitumen partial upgrading over Ag-Ga/ZSM-5 under methane environment. **2017,** *156*, 290-297.

34. Lou, Y.; He, P.; Zhao, L.; Cheng, W.; Song, H. J. A. C. B. E., Olefin Upgrading over Ir/ZSM-5 catalysts under methane environment. **2017,** *201*, 278-289.

35. Lou, Y.; He, P.; Zhao, L.; Song, H. J. F., Refinery oil upgrading under methane environment over PdOx/H-ZSM-5: Highly selective olefin cyclization. **2016,** *183*, 396-404.

36. He, P.; Zhao, L.; Song, H. J. A. C. B. E., Bitumen partial upgrading over Mo/ZSM-5 under methane environment: Methane participation investigation. **2017,** *201*, 438-450.

37. He, P.; Lou, Y.; Song, H. J. F., Olefin upgrading under methane environment over Ag-Ga/ZSM-5 catalyst. **2016,** *182*, 577-587.

38. He, P.; Wen, Y.; Jarvis, J.; Gatip, R.; Austin, D.; Song, H. J. C., Selective Participation of Methane in Olefin Upgrading over Pd/ZSM‐5 and Ir/ZSM‐5: Investigation using Deuterium Enriched Methane. **2017,** *2* (1), 252-256.

39. Wang, A.; He, P.; Yung, M.; Zeng, H.; Qian, H.; Song, H. J. A. C. B. E., Catalytic co-aromatization of ethanol and methane. **2016,** *198*, 480-492.

40. Xiao, Y.; He, P.; Cheng, W.; Liu, J.; Shan, W.; Song, H. J. W. m., Converting solid wastes into liquid fuel using a novel methanolysis process. **2016,** *49*, 304-310.

41. He, P.; Shan, W.; Xiao, Y.; Song, H. J. T. i. C., Performance of Zn/ZSM-5 for in situ catalytic upgrading of pyrolysis bio-oil by methane. **2016,** *59* (1), 86-93.

42. He, P.; Song, H. J. I.; Research, E. C., Catalytic conversion of biomass by natural gas for oil quality upgrading. **2014,** *53* (41), 15862-15870.

43. Lee, D. H.; Song, Y.-H.; Kim, K.-T.; Lee, J.-O. J. P. C.; Processing, P., Comparative study of methane activation process by different plasma sources. **2013,** *33* (4), 647-661.

44. Indarto, A. J. I. T. o. D.; Insulation, E., A review of direct methane conversion to methanol by dielectric barrier discharge. **2008,** *15* (4), 1038-1043.

45. Lee, D. H.; Kim, K.-T.; Song, Y.-H.; Kang, W. S.; Jo, S. J. P. C.; Processing, P., Mapping plasma chemistry in hydrocarbon fuel processing processes. **2013,** *33* (1), 249-269.

46. Reddy, P. V. L.; Kim, K.-H.; Song, H. J. R.; Reviews, S. E., Emerging green chemical technologies for the conversion of CH4 to value added products. **2013,** *24*, 578-585.

47. Heintze, M.; Pietruszka, B. J. C. t., Plasma catalytic conversion of methane into syngas: the combined effect of discharge activation and catalysis. **2004,** *89* (1-2), 21-25.

48. Liu, C.; Marafee, A.; Mallinson, R.; Lobban, L. J. A. c. A., General, Methane conversion to higher hydrocarbons in a corona discharge over metal oxide catalysts with OH groups. **1997,** *164* (1-2), 21-33.

49. Chen, H. L.; Lee, H. M.; Chen, S. H.; Chao, Y.; Chang, M. B. J. A. C. B. E., Review of plasma catalysis on hydrocarbon reforming for hydrogen production—interaction, integration, and prospects. **2008,** *85* (1-2), 1-9.

50. Hao, H.; Wu, B. S.; Yang, J.; Guo, Q.; Yang, Y.; Li, Y. W. J. F., Non-thermal plasma enhanced heavy oil upgrading. **2015,** *149*, 162-173.

51. Taghvaei, H.; Kheirollahivash, M.; Ghasemi, M.; Rostami, P.; Rahimpour, M. R. J. E.; fuels, Noncatalytic upgrading of anisole in an atmospheric DBD plasma reactor: effect of carrier gas type, voltage, and frequency. **2014,** *28* (4), 2535-2543.

52. Jahanmiri, A.; Rahimpour, M.; Shirazi, M. M.; Hooshmand, N.; Taghvaei, H. J. C. e. j., Naphtha cracking through a pulsed DBD plasma reactor: Effect of applied voltage, pulse repetition frequency and electrode material. **2012,** *191*, 416-425.

53. Kong, P. C.; Nelson, L. O.; Detering, B. A., Nonthermal plasma systems and methods for natural gas and heavy hydrocarbon co-conversion. Google Patents: 2005.

54. Luo, Y. R., *Comprehensive handbook of chemical bond energies*. CRC press.: 2007; p 29-38.

55. Nguyen, H. H.; Kim, K.-S., Combination of plasmas and catalytic reactions for CO2 reforming of CH4 by dielectric barrier discharge process. *Catalysis Today* **2015,** *256*, 88-95.

56. Khoja, A. H.; Tahir, M.; Amin, N. A. S., Dry reforming of methane using different dielectric materials and DBD plasma reactor configurations. *Energy Conversion and Management* **2017,** *144*, 262-274.

57. Huang, A.; Xia, G.; Wang, J.; Suib, S. L.; Hayashi, Y.; Matsumoto, H., CO2 Reforming of CH4 by Atmospheric Pressure ac Discharge Plasmas. *Journal of Catalysis* **2000,** *189* (2), 349-359.

58. Mao, S.; Tan, Z.; Zhang, L.; Huang, Q., Plasma-assisted biogas reforming to syngas at room temperature condition. *Journal of the Energy Institute* **2018,** *91* (2), 172-183.

59. Yao, S. L., Ouyang, F., Nakayama, A., Suzuki, E., Okumoto, M., & Mizuno, A. , Oxidative coupling and reforming of methane with carbon dioxide using a high-frequency pulsed plasma. *Energy & Fuels* **2000,** *14* (4), 910-914.

60. Yap, D.; Tatibouët, J.-M.; Batiot-Dupeyrat, C., Catalyst assisted by non-thermal plasma in dry reforming of methane at low temperature. *Catalysis Today* **2018,** *299*, 263-271.

61. Mei, D.; Ashford, B.; He, Y.-L.; Tu, X., Plasma-catalytic reforming of biogas over supported Ni catalysts in a dielectric barrier discharge reactor: Effect of catalyst supports. *Plasma Processes and Polymers* **2017,** *14* (6), 1600076.

62. Mahammadunnisa, S.; Manoj Kumar Reddy, P.; Ramaraju, B.; Subrahmanyam, C., Catalytic Nonthermal Plasma Reactor for Dry Reforming of Methane. *Energy & Fuels* **2013,** *27* (8), 4441-4447.

63. Heintze, M.; Pietruszka, B., Plasma catalytic conversion of methane into syngas: the combined effect of discharge activation and catalysis. *Catalysis Today* **2004,** *89* (1-2), 21-25.

64. Sentek, J.; Krawczyk, K.; Młotek, M.; Kalczewska, M.; Kroker, T.; Kolb, T.; Schenk, A.; Gericke, K.-H.; Schmidt-Szałowski, K., Plasma-catalytic methane conversion with carbon

dioxide in dielectric barrier discharges. *Applied Catalysis B: Environmental* **2010,** *94* (1-2), 19-26.

65. Wang, L.; Yi, Y.; Wu, C.; Guo, H.; Tu, X., One-Step Reforming of CO2 and CH4 into High-Value Liquid Chemicals and Fuels at Room Temperature by Plasma-Driven Catalysis. *Angew Chem Int Ed Engl* **2017,** *56* (44), 13679-13683.

66. Zeng, Y. X.; Wang, L.; Wu, C. F.; Wang, J. Q.; Shen, B. X.; Tu, X., Low temperature reforming of biogas over K-, Mg- and Ce-promoted Ni/Al2O3 catalysts for the production of hydrogen rich syngas: Understanding the plasma-catalytic synergy. *Applied Catalysis B: Environmental* **2018,** *224*, 469-478.

67. Sheng, Z.; Kameshima, S.; Yao, S.; Nozaki, T., Oxidation behavior of Ni/Al2O3 catalyst in nonthermal plasma-enabled catalysis. *Journal of Physics D: Applied Physics* **2018,** *51* (44), 445205.

68. Ray, D.; Reddy, P. M. K.; Subrahmanyam, C., Ni-Mn/γ-Al2O3 assisted plasma dry reforming of methane. *Catalysis Today* **2018,** *309*, 212-218.

69. Mei, D. H.; Liu, S. Y.; Tu, X., CO2 reforming with methane for syngas production using a dielectric barrier discharge plasma coupled with Ni/γ-Al2O3 catalysts: Process optimization through response surface methodology. *Journal of CO2 Utilization* **2017,** *21*, 314-326.

70. Zeng, Y.; Zhu, X.; Mei, D.; Ashford, B.; Tu, X., Plasma-catalytic dry reforming of methane over γ-Al2O3 supported metal catalysts. *Catalysis Today* **2015,** *256*, 80-87.

71. Qi Wang, B.-H. Y., Yong Jin, and Yi Cheng, Dry Reforming of Methane in a Dielectric Barrier Discharge Reactor with Ni/Al2O3 Catalyst: Interaction of Catalyst and Plasma. *Energy & Fuels* **2009,** *23* (8), 4196-4201.

72. Zhang, A.-J.; Zhu, A.-M.; Guo, J.; Xu, Y.; Shi, C., Conversion of greenhouse gases into syngas via combined effects of discharge activation and catalysis. *Chemical Engineering Journal* **2010,** *156* (3), 601-606.

73. Hammer, T.; Kappes, T.; Baldauf, M., Plasma catalytic hybrid processes: gas discharge initiation and plasma activation of catalytic processes. *Catalysis Today* **2004,** *89* (1-2), 5-14.

74. Liu, C.; Yu, K.; Zhang, Y.; Zhu, X.; He, F.; Eliasson, B., Characterization of plasma treated Pd/HZSM-5 catalyst for methane combustion. *Applied Catalysis B: Environmental* **2004,** *47* (2), 95-100.

75. Wang, Z.-j.; Zhao, Y.; Cui, L.; Du, H.; Yao, P.; Liu, C.-j., CO2 reforming of methane over argon plasma reduced Rh/Al2O3 catalyst: a case study of alternative catalyst reduction via non-hydrogen plasmas. *Green Chemistry* **2007,** *9* (6), 554.

76. Krawczyk, K.; Młotek, M.; Ulejczyk, B.; Schmidt-Szałowski, K., Methane conversion with carbon dioxide in plasma-catalytic system. *Fuel* **2014,** *117*, 608-617.

77. Jiang, T., Li, Y., Liu, C. J., Xu, G. H., Eliasson, B., Xue, B., Plasma methane conversion using dielectric-barrier discharges with zeolite A. *Catalysis Today* **2002,** *72* (3-4), 229-235.

78. Baldur Eliasson, C.-j. L., and Ulrich Kogelschatz, Direct Conversion of Methane and Carbon Dioxide to Higher Hydrocarbons Using Catalytic Dielectric-Barrier Discharges with Zeolites. *Industrial & Engineering Chemistry Research* **2000,** *39* (5), 1221-1227.

79. Hosseini, S. E.; Wahid, M. A., Biogas utilization: Experimental investigation on biogas flameless combustion in lab-scale furnace. *Energy Conversion and Management* **2013,** *74*, 426-432.

80. Wang, B., Xu, G., Conversion of methane to C2 hydrocarbons via cold plasma reaction. *Journal of natural gas chemistry* **2003,** *12* (3), 178-182.

81. Liu, C. J., Lobban, L. L., and Mallinson, R. G., Experimental investigations on the interaction between plasmas and catalyst for plasma catalytic methane conversion (PCMC) over zeolites. *In Studies in surface science and catalysis* **1998,** *119*, 361-366.

82. Ashok, B.; Denis Ashok, S.; Ramesh Kumar, C., LPG diesel dual fuel engine – A critical review. *Alexandria Engineering Journal* **2015,** *54* (2), 105-126.

83. Maclaine-Cross, I. L., Leonardi, E. In *Performance and safety of LPG refrigerants*, Fuel for Change, Australia, Surfers, Australian Liquefied Petroleum Gas Association Ltd: Australia, Surfers, 1995; pp 149-168.

84. Maitra, A., Critical performance evaluation of catalysts and mechanistic implications for oxidative coupling of methane. *Applied Catalysis A: General* **1993,** *104* (1), 11-59.

85. Periana, R. A.; Bhalla, G.; Tenn III, W. J.; Young, K. J.; Liu, X. Y.; Mironov, O.; Jones, C.; Ziatdinov, V. R., Perspectives on some challenges and approaches for developing the next generation of selective, low temperature, oxidation catalysts for alkane hydroxylation based on the CH activation reaction. *Journal of Molecular Catalysis A: Chemical* **2004,** *220* (1), 7-25.

86. Rahimi, N.; Moradi, D.; Sheibak, M.; Moosavi, E.; Karimzadeh, R., The influence of modification methods on the catalytic cracking of LPG over lanthanum and phosphorus modified HZSM-5 catalysts. *Microporous and Mesoporous Materials* **2016,** *234*, 215-223.

87. Zhang, Q., Liu, Y., Huang, J., Qian, W., Wang, Y., Wei, F. , Synthesis of single-walled carbon nanotubes from liquefied petroleum gas. *Nano.* **2008,** *3* (2), 95-100.

88. Laosiripojana, N.; Sutthisripok, W.; Charojrochkul, S.; Assabumrungrat, S., Steam reforming of LPG over Ni and Rh supported on Gd-CeO2 and Al2O3: Effect of support and feed composition. *Fuel* **2011,** *90* (1), 136-141.

89. Anunziata, O. A., Pierella, L. B. , Zn-ZSM-11 zeolite catalyst for LPG aromatization. *Catalysis letters* **1992,** *16* (4), 437-441.

90. Al‐Zahrani, S. M., Catalytic Conversion of LPG to High‐Value Aromatics: The Current State of the Art and Future Predictions. *Developments in Chemical Engineering and Mineral Processing* **1998,** *6* (1-2), 101-120.

91. Anunziata, O. A., Eimer, G. A., Pierella, L. B., Catalytic conversion of natural gas with added ethane and LPG over Zn-ZSM-11. *Applied Catalysis A: General,* **2000,** *190* (1-2), 169-176.

92. Giannetto, G.; Monque, R.; Galiasso, R., Transformation of LPG into Aromatic Hydrocarbons and Hydrogen over Zeolite Catalysts. *Catalysis Reviews* **1994,** *36* (2), 271-304.

93. Spivey, J. J.; Hutchings, G., Catalytic aromatization of methane. *Chem. Soc. Rev.* **2014,** *43* (3), 792-803.

94. Yuliati, L.; Yoshida, H., Photocatalytic conversion of methane. *Chem Soc Rev* **2008,** *37* (8), 1592-602.

95. Chen, X.; Li, Y.; Pan, X.; Cortie, D.; Huang, X.; Yi, Z., Photocatalytic oxidation of methane over silver decorated zinc oxide nanocatalysts. *Nat Commun* **2016,** *7*, 12273.

96. Yuliati, L.; Hattori, T.; Itoh, H.; Yoshida, H., Photocatalytic nonoxidative coupling of methane on gallium oxide and silica-supported gallium oxide. *Journal of Catalysis* **2008,** *257* (2), 396-402.

97. Li, L.; Li, G. D.; Yan, C.; Mu, X. Y.; Pan, X. L.; Zou, X. X.; Wang, K. X.; Chen, J. S., Efficient sunlight-driven dehydrogenative coupling of methane to ethane over a Zn(+)-modified zeolite. *Angew Chem Int Ed Engl* **2011,** *50* (36), 8299-303.

98. Villa, K.; Murcia-López, S.; Andreu, T.; Morante, J. R., Mesoporous WO3 photocatalyst for the partial oxidation of methane to methanol using electron scavengers. *Applied Catalysis B: Environmental* **2015,** *163*, 150-155.

99. Shimura, K.; Yoshida, H., Hydrogen production from water and methane over Pt-loaded calcium titanate photocatalyst. *Energy & Environmental Science* **2010,** *3* (5), 615-617.

100. Carman, R.; Mildren, R.; Ward, B.; Kane, D., High-pressure (> 1 bar) dielectric barrier discharge lamps generating short pulses of high-peak power vacuum ultraviolet radiation. *Journal of Physics D: Applied Physics* **2004,** *37* (17), 2399.

101. El-Dakrouri, A.; Yan, J.; Gupta, M.; Laroussi, M.; Badr, Y., VUV emission from a novel DBD-based radiation source. *Journal of Physics D: Applied Physics* **2002,** *35* (21), L109.

102. Kanakaraju, D.; Kockler, J.; Motti, C. A.; Glass, B. D.; Oelgemöller, M., Titanium dioxide/zeolite integrated photocatalytic adsorbents for the degradation of amoxicillin. *Applied Catalysis B: Environmental* **2015,** *166*, 45-55.

103. Zhang, X.; Zhou, M.; Lei, L., Preparation of anatase TiO2 supported on alumina by different metal organic chemical vapor deposition methods. *Applied Catalysis A: General* **2005,** *282* (1-2), 285-293.

104. Sentek, J.; Krawczyk, K.; Młotek, M.; Kalczewska, M.; Kroker, T.; Kolb, T.; Schenk, A.; Gericke, K.-H.; Schmidt-Szałowski, K. J. A. C. B. E., Plasma-catalytic methane conversion with carbon dioxide in dielectric barrier discharges. **2010,** *94* (1-2), 19-26.

105. Tu, X.; Whitehead, J. J. A. C. B. E., Plasma-catalytic dry reforming of methane in an atmospheric dielectric barrier discharge: Understanding the synergistic effect at low temperature. **2012,** *125*, 439-448.

106. Lovestead, T. M.; Bruno, T. J. J. E.; Fuels, Application of the advanced distillation curve method to the aviation fuel avgas 100LL. **2009,** *23* (4), 2176-2183.

107. Luo, Y.-R., *Handbook of bond dissociation energies in organic compounds*. CRC press: 2002.

108. El-Dakrouri, A.; Yan, J.; Gupta, M.; Laroussi, M.; Badr, Y. J. J. o. P. D. A. P., VUV emission from a novel DBD-based radiation source. **2002,** *35* (21), L109.

APPENDIX: LIST OF PUBLICATIONS AND PATENT FILING/APPLICATION

Journal Publications:

1. Wang, A., Harrhy, J., Meng, S., He, P., Liu, L., **Song, H.***, "Nonthermal Plasma-Catalytic Conversion of Biogas to Liquid Chemicals with Low Coke Formation", *Energy Conversion & Management*, (**2019**), 191, 93-101
2. Wang, A., Meng, S., **Song, H.***, "Non-thermal plasma induced photocatalytic conversion of light alkanes into high value-added liquid chemicals at near ambient conditions", *Chemical Communications*, (**2020**), 56, 5263-5266
3. Meng, S., Wang, A., He, P., **Song, H.***, "Non-thermal plasma assisted photocatalytic conversion of simulated natural gas for high quality gasoline production near ambient conditions", *The Journal of Physical Chemistry Letters*, (**2020**), 11, 3877-3881